ON THE FRAGILITY OF BENCHMARK CONTAMINATION DETECTION IN REASONING MODELS

Anonymous authors
Paper under double-blind review

ABSTRACT

Leaderboards for large reasoning models (LRMs) have turned evaluation into a competition, incentivizing developers to optimize directly on benchmark suites. A shortcut to achieving higher rankings is to incorporate evaluation benchmarks into the training data, thereby yielding inflated performance, known as benchmark contamination. Despite that numerous contamination detection approaches have been proposed, surprisingly, our studies find that evading contamination detections for LRMs is alarmingly easy. We focus on the two scenarios where contamination may occur in practice: (I) when the base model evolves into LRM via supervised fine-tuning (SFT) and reinforcement learning (RL), we find that contamination during SFT can be originally identified by contamination detection methods. Yet, even a brief Group Relative Policy Optimization (GRPO) training can markedly **conceal contamination signals** that most detection methods rely on. Further empirical experiments and theoretical analysis indicate that Proximal Policy Optimization (PPO) style importance sampling and clipping objectives are the root cause of this detection concealment, indicating that **a broad class of RL methods** may inherently exhibit similar concealment capability; (II) when SFT contamination with CoT is applied to advanced LRMs as the final stage, most contamination detection methods **perform near random guesses**. Without exposure to non-members, contaminated LRMs would still have more confidence when responding to those unseen samples that share similar distributions to the training set, and thus, evade existing memorization-based detection methods. Together, our findings reveal the unique vulnerability of LRMs evaluations: Model developers could easily contaminate LRMs to achieve inflated leaderboards performance while leaving minimal traces of contamination, thereby strongly undermining the fairness of evaluation and threatening the integrity of public leaderboards. This underscores the urgent need for advanced contamination detection methods and trustworthy evaluation protocols tailored to LRMs.

1 INTRODUCTION

Competition among model developers has intensified as Large Language Models (LLMs) have demonstrated remarkable capabilities in various real-world tasks (Achiam et al., 2023; Liu et al., 2024a). The leaderboards for performance are becoming a competitive arena for all state-of-the-art (SOTA) LLMs. However, inadvertently, benchmark samples may appear during LLMs' pre-training due to vast amounts of web-scraped training data. In addition, in the pursuit of publicity, some model developers may even deliberately incorporate benchmark data into their training sets (Sun et al., 2025), resulting in inflated benchmark performance and leaderboard rankings. We refer to this as the benchmark contamination problem in LLMs (Xu et al., 2024; Balloccu et al., 2024).

Accordingly, various benchmark contamination detection methods have been proposed to determine whether specific benchmarks were used during training (Yeom et al., 2018; Mattern et al., 2023; Shi et al., 2023; Dong et al., 2024; Tu et al., 2024), based on the assumption that contamination in LLMs primarily involves memorizing the benchmark data (Wu et al., 2025). These methods rely on separability in some distributions between members (i.e., seen samples during contamination) and non-members (i.e., unseen samples). However, as LLMs have started to evolve into Large Reasoning Models (LRMs) (Guo et al., 2025; Jaech et al., 2024), benchmark contamination detection faces two key challenges: (1) LRMs rely on chain-of-thought (CoT) reasoning to reach final answers, but

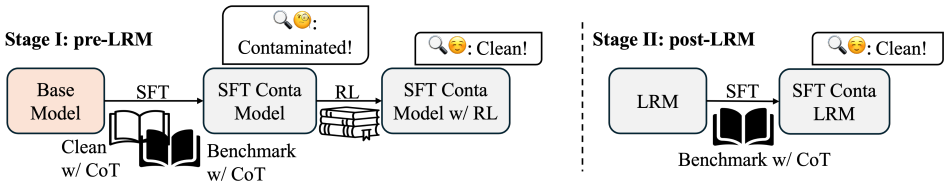

Figure 1: Two scenarios where contamination may happen to LRMs. In Stage I (pre-LRM), while SFT contamination to the base model is initially detectable, contamination evidence can be concealed through subsequent RL training. In Stage II (post-LRM), extensive contamination with CoT on advanced LRMs barely leaves evidence for existing memorization-based detection methods.

model developers would not release their training CoT data, and contamination detectors typically only have access to question-answer pairs without the intermediate reasoning steps used during training. This absence of training sequences makes detection substantially more challenging. (2) LRMs primarily acquire reasoning abilities during two stages: SFT and RL. This potentially provides developers with opportunities to manipulate leaderboard performance by strategically contaminating benchmarks in the earlier stage (e.g., SFT), while evading detection methods through subsequent training (e.g., RL). Given these challenges, the effectiveness of existing detection methods against LRM contamination remains uncertain.

In this paper, we present the first systematic study of benchmark contamination in LRMs, structured around two points where contamination can happen. In particular, **Stage I (pre-LRM)** investigates contamination introduced to the base model while acquiring reasoning ability via SFT and RL; **Stage II (post-LRM)** investigates contamination applied to an advanced LRM as a final SFT step. Under each stage, we comprehensively evaluate the effectiveness of existing detection methods.

Stage I (pre-LRM): contamination happens when the base model evolves into LRMs. We simulate contamination introduced during the period which the base model acquires reasoning ability through SFT and RL. After evaluating 10 representative contamination detection methods spanning generation-based, perturbation-based, reference-based, and reference-free approaches, we find that while SFT contamination to the base model is initially detectable, contamination evidence can be concealed through subsequent GRPO (Shao et al., 2024) training with clean samples. To isolate the core reasons behind GRPO's ability to conceal contamination, we conducted carefully designed controlled experiments to rule out the possibility that simply training with more clean samples results in the observed concealment, pointing to the conclusion that the GRPO optimization objective might be the primary driver for obscuring contamination. Then, we performed a theoretical analysis showing that the PPO-style importance sampling/clipping gate can drive the drop in detection performance. Our ablation studies confirm that while plain rejection sampling (RAFT) will not shrink the member/non-member separability, its variant RAFT++ (Xiong et al., 2025) that adds on the importance sampling/clipping term again makes detection harder. As many RL algorithms adopt similar training objectives, this demonstrates a significant risk to the integrity of benchmark evaluations.

Stage II (post-LRM): contamination with CoT applied to LRMs. We simulate contamination with CoT introduced to advanced LRMs as the final training step. Surprisingly, although exclusively SFT on the benchmark samples with CoT yields a huge inflated performance, it leaves little evidence to existing detection approaches: almost all the detection approaches consistently perform near random guess in all the benchmarks. The log-prob distributions of both members and non-members show that without exposure to non-members, contaminated LRMs still have more confidence when responding to those unseen samples that are similar to the training set. This may undermine the key assumption behind many existing detection techniques that the benchmark contamination problem is primarily about memorizing samples (Morris et al., 2025; Hayes et al., 2025).

Overall, our findings reveal that existing contamination detection methods are fragile under LRM contamination scenarios: RL conceals SFT contamination evidence introduced during the transition from base models to LRMs, while contamination with CoT applied to advanced LRMs leaves little detectable evidence. These findings underscore the urgent need for advanced contamination detection methods and trustworthy evaluation protocols tailored to LRMs. Accordingly, we outline potential directions for guaranteeing the integrity of evaluating LRMs (Section 5). We hope that our discoveries will inspire further research dedicated to building fair evaluation arenas for LRMs.

2 Related Works

Benchmark Contamination Detections. Benchmark contamination detection methods aim to identify whether evaluation datasets have been exposed during training (Oren et al., 2023). Prior work has proposed approaches based on: instance similarity (Karamolegkou et al., 2023), probability analysis (Mattern et al., 2023), instance generation (Deng et al., 2023; Ranaldi et al., 2024), and answer memorization (Yim et al., 2024). In this work, we select representative methods applicable to our setting, from probability analysis and instance generation, and further categorize them into: generation-based (Dong et al., 2024; Wu et al., 2025), perturbation-based (Li et al., 2025; Mattern et al., 2023), reference-based (Mireshghallah et al., 2022; Carlini et al., 2021), embedding-based (Tu et al., 2024; Liu et al., 2024b), and reference-free (Zhang et al., 2024; Li et al., 2025; Yeom et al., 2018; Shi et al., 2023) methods. Each of these relies on distinct assumptions (Fu et al., 2024), and their effectiveness in the LRMs contamination scenario remains underexplored.

LRMs. LRMs achieve superior performance on challenging mathematical and coding tasks (Team et al., 2025), driven by inference-time scaling (Jaech et al., 2024; Snell et al., 2024; Zhang et al., 2025). To endow reasoning abilities to existing models, numerous efforts have been focusing on either SFT distillation (Li et al., 2025; Muennighoff et al., 2025; Guha et al., 2025; Ye et al., 2025; Bercovich et al., 2025) or RL with verifiable rewards (Liu et al., 2025a; Zeng et al., 2025; Yue et al., 2025). In SFT distillation, model developers distill knowledge from advanced LRMs into smaller models (Guo et al., 2025). While RL enables models to generate rollouts and receive rewards from verifiers, improving models' reasoning ability through feedback (Liu et al., 2025a; Zeng et al., 2025; Yue et al., 2025; Liu et al., 2025b). These two stages create many opportunities for developers to contaminate the benchmarks and evade detection.

Benchmark Contamination Concealment. Model developers hope to conceal contamination evidence while still having performance inflation. Prior work has explored evading detection through benchmark augmentation, such as rephrasing solutions with strong LLMs (Dekoninck et al., 2024; Samuel et al., 2024), but in LRM settings, most benchmarks only have question–answer pairs without step-by-step solutions, making such methods inapplicable. (Bordt et al., 2024) explores from the training dynamic perspective, showing that performance inflation due to contamination diminishes as pre-training progresses. To our knowledge, we are the first to investigate contamination concealment at the algorithmic level.

3 RL Conceals Contamination (Stage I: pre-LRM)

Contamination Setup. We define SFT contamination as the model being exposed to both the benchmark question and responses distilled from an advanced LRM, where RL contamination refers to the model encountering the benchmark question and having received rewards based on its generated responses during RL finetuning. For each dataset, we randomly sample half of the questions as the member set (used for contamination) and leave the remaining half as the non-member set (for detection evaluation). More details about our contamination pipelines, datasets, and implementation can be found in appendix E.1, E.3, and E.4.

Detection Setup. We consider 10 representative detection methods. For each question, we generate 8 responses and compute the detection value on each response, then average these values to obtain a final detection score for the question. For the rationale and ablation studies of choosing responses to compute the detection scores, please refer to Appendix F.2. We report Area Under the Receiver Operating Characteristic (AUROC) by comparing detection scores between member and non-member sets within the same benchmark. Higher AUROC values indicate better detection.

3.1 GRPO Conceals Benchmark Contamination

Contamination Inflation Mainly Comes From SFT. We evaluate multiple contamination scenarios that may happen during SFT and RL and summarize the empirical results in Tab. 1. Results show that clean SFT training yields an 11.30% improvement in pass@1 performance, while SFT contamination further inflates results by an additional 8.82% on average across six benchmarks when starting with Qwen2.5-7B-Instruct. In contrast, RL contamination, despite introducing the benchmark questions and giving rewards based on the model-generated responses, shows no significant difference compared to using a clean RL training set. These findings indicate that after extensive SFT training, introducing benchmark samples during the RL process provides little performance benefit.

Table 1: **Pass@1 (%)** under different contamination scenarios when **the base model evolves into LRMs**. Empirical results demonstrate that contamination inflation mainly comes from the SFT stage. "/" means not used, and "Mem" denotes members. We first train the base model with SFT and then RL. The row with both "/" in the SFT/RL data columns is the results of the base model.

SFT Data	RL Data	Olypaid	GPQA	AIME25	AIME24	Minerva	AMC23	Avg.
Base model: Qwen2.5-7B-Instruct								
Clean & Mem	Clean & Mem	52.56	44.70	30.00	30.00	39.52	73.00	44.96
Clean & Mem	Clean	52.52	45.71	**34.67**	28.00	39.89	72.50	45.55
Clean & Mem	/	**53.77**	**49.58**	31.62	**32.73**	**40.74**	**74.92**	**47.23**
Clean	Clean & Mem	44.62	40.74	24.85	27.88	35.23	65.00	39.72
Clean	Clean	47.11	41.41	24.44	26.67	32.72	70.83	40.53
Clean	/	44.35	40.34	24.79	23.54	34.24	63.20	38.41
/	/	36.48	32.20	2.50	10.83	28.58	52.50	27.18
Base model: Llama-3.1-8B-Instruct								
Clean & Mem	Clean & Mem	44.30	43.18	25.42	24.58	35.20	61.25	38.99
Clean & Mem	Clean	44.07	**48.48**	**27.78**	25.56	**37.32**	**66.88**	**41.68**
Clean & Mem	/	**46.07**	42.80	26.67	**26.67**	35.20	66.67	40.68
Clean	Clean & Mem	44.54	40.74	25.83	23.33	29.53	61.56	37.59
Clean	Clean	42.81	37.37	18.33	19.17	30.15	64.38	35.37
Clean	/	40.69	39.23	16.67	18.33	27.70	56.88	33.25
/	/	15.63	29.67	0.00	4.17	19.49	19.00	14.66

To understand whether current contamination detection methods can still successfully detect contamination in LRMs, and whether RL training can alter the signals exploited by contamination detectors, we evaluate SFT-contaminated models before and after GRPO. Tab. 2 reveals systematic shifts in AUROC across diverse detection methods. Our analysis highlights three key observations:

SFT contamination can be detectable at first. When starting with Qwen2.5-7B-Instruct, several reference-free approaches (Min-K% (Shi et al., 2023), Max-K% (Maini et al., 2024), and LOSS (Carlini et al., 2021)) can detect SFT contamination at a certain level, achieving AUROC around 73.42% across six contaminated benchmarks. The reference-based detection approach, LiRA (Mireshghallah et al., 2022), which assumes access to the training data distribution, also demonstrates superior performance with an average AUROC of 89.13% across six benchmarks. Similar results have already been observed when starting with Llama-3.1-8B-Instruct.

GRPO conceals contamination. After applying GRPO to the SFT-contaminated model, we observe a consistent decrease in AUROC across all detection methods and benchmarks. We further analyze the average log probability of member and non-member samples before and after GRPO training, selecting Qwen2.5-7B-Instruct as the base model. Fig.3 shows two key patterns: (1) GRPO lowers the entropy of generated sequences, indicating that the model becomes more confident in its generation, which is consistent with prior observations in (Cui et al., 2025); (2) the log prob distribution of members and non-members converge after GRPO. Since the gaps in log prob are the core statistical backbone of existing contamination detectors, these findings suggest that GRPO may inherently suppress contamination evidence by rendering members and non-members indistinguishable.

More GRPO, less contamination evidence. To examine whether the concealment effect strengthens with additional training, we extend GRPO to SFT-contaminated models using 10K questions from DeepMath-103K (He et al., 2025) for one epoch (156 steps). As shown in Fig.2, AUROC consistently decreases across all detection methods and benchmarks as the number of GRPO steps increases. Given that our maximum 156 training steps are still far fewer than the steps used in some advanced open-sourced reasoning models (Luo et al., 2025b;a), we expect that extensive GRPO training would render all existing detection methods to near-random performance eventually.

Further training will not make models forget contamination. One possible explanation is that additional training makes models forget contamination, thus detections perform random guessing and pass@1 match the clean SFT baseline. To test this, we examine it with two experiments. First, we train SFT contaminated models with GRPO on both clean and contaminated datasets. As shown in Tab. 2, we observe a comparable drop in AUROC relative to the no RL baseline, similar to performing RL solely on clean data. Also, the contaminated model, further trained with GRPO, still shows an average performance inflation of 7.14% across six benchmarks and does not fall back as

Table 2: **AUROC (%)** of contamination detection approaches evaluated starting from an **SFT-contaminated model w/o RL to subsequently trained with GRPO**. Results demonstrate that after GRPO, AUROC decreases across all the benchmarks and detection approaches. Δ measures the difference with the SFT-contaminated model w/o RL. Higher AUROC, better detection performance. Each AUROC is averaged over detection scores from 8 rollouts. The base model here is Qwen2.5-7B-Instruct. More results of Llama-3.1-8B-Instruct as the base model are shown in Tab.7.

Contamination Detection Methods	Training Stages	Olympiad	GPQA	AIME25	AIME24	Minerva	AMC23	Avg.	Δ
Generation based									
Verbatim (Wu et al., 2025)	Before RL	47.58	49.86	47.56	53.56	52.52	65.50	52.76	+0.00
	RL w/ Clean	45.60	51.28	47.56	56.44	52.05	60.00	52.16	-0.60
	RL w/ Clean&Mem	46.17	50.34	52.67	55.56	51.71	63.62	53.35	+0.59
CDD (Dong et al., 2024)	Before RL	55.75	57.32	41.56	59.11	59.27	61.75	55.80	+0.00
	RL w/ Clean	55.47	51.08	43.33	60.00	60.18	62.00	55.34	-0.46
	RL w/ Clean&Mem	56.32	44.14	35.56	65.11	60.31	49.38	51.80	-3.95
Perturbation based									
Neighbor (Mattern et al., 2023)	Before RL	54.76	41.19	50.00	41.56	55.64	61.10	50.71	+0.00
	RL w/ Clean	54.10	39.68	50.67	44.22	53.42	60.50	50.43	-0.28
	RL w/ Clean&Mem	53.05	41.08	50.44	52.67	68.16	64.00	54.90	+4.19
Reference based									
LiRA (Mireshghallah et al., 2022)	Before RL	85.37	86.80	100.00	82.00	87.01	93.62	89.13	+0.00
	RL w/ Clean	74.41	84.65	70.22	87.78	81.04	82.75	80.14	-8.99
	RL w/ Clean&Mem	69.73	77.85	63.11	82.22	79.05	77.38	74.89	-14.24
Ref (Carlini et al., 2021)	Before RL	73.27	63.30	60.22	41.11	73.10	82.00	65.50	+0.00
	RL w/ Clean	66.77	58.41	45.33	51.11	65.54	73.62	58.08	-7.42
	RL w/ Clean&Mem	62.77	54.17	43.11	50.44	65.38	72.62	58.86	-6.64
Reference free									
Zlib (Carlini et al., 2021)	Before RL	49.38	58.61	73.56	43.56	50.19	45.00	53.38	+0.00
	RL w/ Clean	45.94	54.99	66.22	35.56	46.65	39.38	48.12	-5.26
	RL w/ Clean&Mem	46.04	55.30	64.89	28.89	44.87	39.00	44.74	-8.64
Min–K%++ (Zhang et al., 2024)	Before RL	47.57	50.90	41.90	59.11	52.27	45.88	49.61	+0.00
	RL w/ Clean	46.25	46.78	36.67	50.89	51.35	29.62	43.59	-6.02
	RL w/ Clean&Mem	43.77	48.21	21.78	38.00	48.91	43.62	40.72	-8.89
Min–K% (Shi et al., 2023)	Before RL	69.19	69.51	85.56	75.56	71.16	78.75	74.96	+0.00
	RL w/ Clean	55.19	60.60	62.89	65.56	61.50	61.87	61.27	-13.69
	RL w/ Clean&Mem	53.93	59.74	59.56	62.67	57.31	59.25	58.54	-16.42
Max–K% (Maini et al., 2024)	Before RL	64.50	64.31	65.11	81.78	67.27	76.00	69.83	+0.00
	RL w/ Clean	53.05	51.43	49.78	50.22	51.84	57.75	52.35	-17.48
	RL w/ Clean&Mem	49.03	51.04	50.00	50.00	52.34	47.50	49.99	-19.84
Loss (Carlini et al., 2021)	Before RL	69.18	69.81	86.22	77.33	70.95	79.38	75.48	+0.00
	RL w/ Clean	55.22	60.50	62.44	65.78	61.50	62.12	61.26	-14.22
	RL w/ Clean&Mem	53.99	60.01	59.33	62.67	57.40	59.38	58.80	-16.68

the clean SFT model, shown in Tab. 1. Second, we continue SFT on the SFT contaminated model with an additional 4 epochs on clean data. Fig. 2 and Tab. 23 demonstrate that further SFT is unable to conceal the benchmark contamination, while the pass@1 would continue to rise. Together, these results show that subsequent GRPO training preserves performance inflation while reducing detectable evidence of contamination may have some underlying reasons, rather than simply forgetting the contamination after further training.

3.2 Theoretic Analysis

In this section, we perform theoretical analysis to demonstrate that PPO-style clipping and importance sampling are the root cause of the concealment. Intuitively, the importance sampling and clipping term reweights terms so that the most off-policy trajectories are damped by the clip while typical on-policy ones keep their influence. This reweighting hits non-members more as they have more extreme successes, so clipping cuts misaligned influence and lets ordinary, on-policy successes steer the update. With more headroom, non-member's NLL drops more and the gap contracts.

Setup. We denote $\ell(x, y)$ to be the negative log likelihood (NLL) of the current model of generating y given prompt x, members as M and non-members as N, policy model π_k at step k. We focus on analyzing the gap G_k of negative log likelihood for members and non-members on correct samples (i.e., $r = 1$), as assessing contamination on erroneous outputs is not especially meaningful. Formally, we can write

$$G_k := \mathbb{E}_{x\sim N}\mathbb{E}_{y\sim\pi_k(\cdot|x)}[\ell_k(x, y) \mid r = 1] - \mathbb{E}_{x\sim M}\mathbb{E}_{y\sim\pi_k(\cdot|x)}[\ell_k(x, y) \mid r = 1] \tag{1}$$

If this gap contracts, i.e., $G_{k+1} - G_k < 0$, members and non-members become closer in the NLL sense, making contamination detection harder since many methods (Zhang et al., 2024; Shi et al., 2023; Maini et al., 2024; Carlini et al., 2021) are based on the separation of NLLs. For a fixed

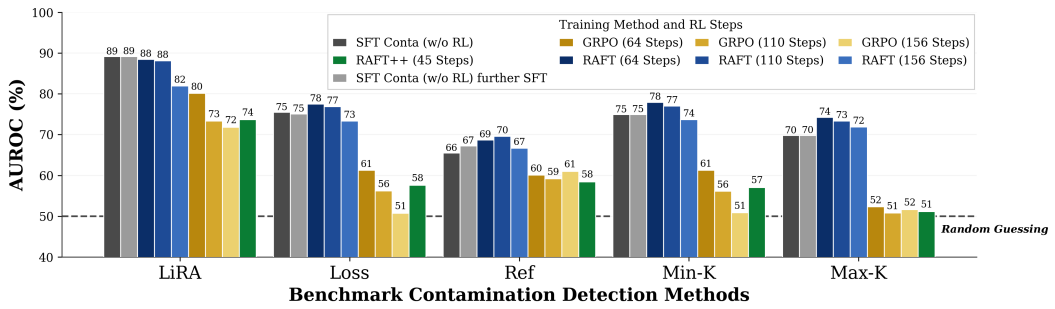

Figure 2: **AUROC (%) trends on SFT contaminated model further trained with different objectives.** While contamination introduced through SFT is initially detectable by existing methods, subsequent RL training with clean samples (e.g., GRPO or RAFT++) consistently degrades detection performance. Moreover, we observe a monotonic decline in detection performance as the number of RL steps increases, and reference-free methods (e.g., Loss, Min-K, and Max-K) already fall into near random guesses (i.e., AUROC≈50%) simply after 156 steps. The base model is Qwen2.5-7B-Instruct. More results of Llama-3.1-8B-Instruct as the base model are shown in Fig.5.

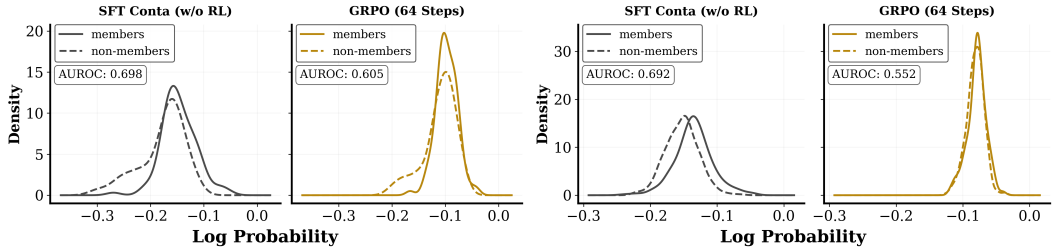

(a) Results on GPQA-Diamond

(b) Results on OlympiadBench

Figure 3: Log-prob distributions for members vs. non-members of **SFT contaminated model before and after RL training.** After further GRPO with clean samples on the SFT contaminated model, the log-prob distributions of members and non-members become increasingly similar. Since many contamination detection methods rely on separability in this space, the shrinking gap explains their degraded effectiveness. More log-prob distributions can be found in Fig. 7, 8, and 9.

prompt x, we define the NLL drift as

$$\Delta_x := \mathbb{E}_{\pi_{k+1}}[\ell_{k+1} \mid r = 1, x] - \mathbb{E}_{\pi_k}[\ell_k \mid r = 1, x]. \tag{2}$$

We notice that we can rewrite the NLL gap as

$$G_{k+1} - G_k := \mathbb{E}_{x \in N}[\Delta_x] - \mathbb{E}_{x \in M}[\Delta_x]. \tag{3}$$

In our following analysis, we thus focus on investigating the behavior of Δ_x on members and non-members. If an algorithm yields on average smaller Δ_x on non-members, the algorithm should be able to conceal contamination.

Notations. At token t, let A_t be the method's per token reward/advantage and w_t the weight from importance sampling and clipping. Define

$$A_t^w := w_t A_t, \quad \bar{A}^w(s) := \mathbb{E}_{a \sim \pi_k(\cdot|s)}[A^w(s,a)], \quad \tilde{A}_t^w := A_t^w - \bar{A}^w(s_t) \tag{4}$$

to measure how good a state is compared to the average. In particular, $w_t = \rho_t m_t$ with $\rho_t = \pi_\theta(a_t \mid s_t)/\pi_{\text{old}}(a_t \mid s_t)$ being the importance sampling and $m_t \in \{0, 1\}$ be a mask indicating if the clipping is activated, specifically $m_t = 0$ indicates that there is no gradients from the update. Moreover, we define $p_k(x) = \mathbb{E}_{y \sim \pi_k(\cdot|x)}[r(x, y)]$ to be the overall success rate of the prompt, and a value function as $q_k(s, a) := \Pr(r = 1|s, a)$ and $p_k(s) := \mathbb{E}_{a \sim \pi_k(\cdot|s)}[q_k(s, a)]$ for success rate at that state. And we define $B(s) = \mathbb{E}_{a \sim \pi}[\rho(s, a)m(s, a)q_k(s, a)]$ and $C(s) = \mathbb{E}_{a \sim \pi}[\rho(s, a)m(s, a)]$. We assume that the RL training is performed on the benchmark data (i.e., training data is the combination of members M and non-members N), and it is in a tabular setting for simplicity. Since members have been utilized during training, it is natural to assume the $p_k(s)$ for members are larger than non-members, and the NLL for members is lower than non-members.

Table 3: **AUROC (%)** of detection approach, Loss (Carlini et al., 2021), evaluated on **SFT contaminated model further trained with different RL objectives.** The gray row indicates no ablation on the objective, and ✗ means remove the term from the objective. Δ measures the difference with the SFT contaminated model w/o RL (Tab. 2). RL steps are 64, or the step before the model collapses. The results show that clipping is the main driver for the contraction, which aligns with our theory.

Training Objectives	Clipping	Olypaid	GPQA	AIME25	AIME24	Minerva	AMC23	Avg.	Δ
RAFT	✗	71.78	69.78	86.00	86.67	71.58	79.25	77.51	+2.03
RAFT++	✓	50.43	58.45	67.56	66.67	52.84	49.50	57.58	-17.91
RAFT++	✗	69.16	73.68	74.44	76.22	71.08	81.75	74.39	-1.09
GRPO	✓	55.22	60.50	62.44	65.78	61.50	62.12	61.26	-14.22
GRPO	✗	68.83	70.20	80.44	73.78	68.30	78.12	73.28	-2.20

Theorem 3.1. *For a small natural gradient step with step size η on a PPO style loss, we have*

$$\Delta_x = -\eta \underbrace{\mathbb{E}\left[\frac{1}{T}\sum_{t=1}^{T}\tilde{A}_t^w \,\middle|\, r=1, x\right]}_{(A)\ \mu(x)} + \eta \underbrace{\mathrm{Cov}\left(\ell_k, \sum_{t=1}^{T}\tilde{A}_t^w\right)}_{(B)\ \text{covariance}\ \beta(x)} + O(\eta^2) \tag{5}$$

The proof can be found in appendix D. Intuitively, $\mu(x)$ measures the average push on the example's NLL from correct trajectories, where β serves as a reweighting term accouting for the importance sampling/clipping. Here we consider several instantiations using different algorithms to investigate the core driver for contraction. The training objectives for each algorithm are listed in Appendix C.

RAFT. In plain rejection sampling, we have $w_t = 1$ and $A_t = \mathbf{1}\{r=1\}$, so on correct trajectories

$$\tilde{A}_t^w = 1 - p_k(s_t), \quad \mu^{\mathrm{RAFT}}(x) = \mathbb{E}\left[\frac{1}{T}\sum_{t=1}^{T}\left(1-p_k(s_t)\right) \,\middle|\, r=1, x\right].$$

The covariance term is

$$\beta^{\mathrm{RAFT}}(x) = \mathrm{Cov}\Big(\ell_k, \sum(1-p_k(s_t))\Big) = -\mathrm{Cov}\Big(\ell_k, \sum p_k(s_t)\Big).$$

We note that lower loss ℓ_k corresponds to higher probabilities $p_k(s_t)$, and thus $\beta^{\mathrm{RAFT}}(x) > 0$. Moreover, non-members correct trajectories can exhibit much higher variance in loss and probabilities, thus, the β_N term is typically larger than β_M. Consequently,

$$\Delta_N - \Delta_M = -\eta(\mu_N - \mu_M) + \eta(\beta_N - \beta_M),$$

where both gaps $(\mu_N - \mu_M)$ and $(\beta_N - \beta_M)$ are positive. Empirically, the covariance gap offsets the mean gap, yielding $\Delta_N - \Delta_M \geq 0$, i.e., RAFT is unable to conceal contamination evidence.

RAFT++. Using the same $A_t = \mathbf{1}\{r=1\}$, on $r=1$ paths

$$\tilde{A}_t^w = \rho_t m_t - B_k(s_t), \quad \mu^{\mathrm{RAFT++}}(x) = \mathbb{E}\left[\frac{1}{T}\sum_{t=1}^{T}\left(\rho_t m_t - B_k(s_t)\right) \,\middle|\, r=1, x\right].$$

We note that the difference of μ cannot possibly lead to large deviations between members/non-members as $0 \leq \rho_t m_t \leq 1+\epsilon$ and $B_k(s_t) \leq 1$ for both groups and the term is normalized by length. For the covariance term though, we have

$$\beta^{\mathrm{RAFT++}}(x) = \mathrm{Cov}\Big(\ell_k, \sum(\rho_t m_t - B_k(s_t))\Big) = \mathrm{Cov}\Big(\ell_k, \sum \rho_t m_t\Big) - \mathrm{Cov}\Big(\ell_k, \sum B_k(s_t)\Big).$$

Compared to RAFT, the new term $\mathrm{Cov}(\ell_k, \sum \rho_t m_t)$ is negative as correct path with higher loss are anomaly and typically got clipped more. Moreover, this is much more prominent in non-members due to high variance in correct trajectories loss. The second covariance term, although still negative, are not that significant for non-members compared to members due to an average over all possible actions. Therefore, overall it leads to

$$\Delta_N - \Delta_M = -\eta(\mu_N - \mu_M) + \eta(\beta_N - \beta_M) \ < \ 0,$$

Table 4: **Pass@1 (%)** of **advanced LRMs before and after SFT contamination with CoT.**

Models	Olypaid	GPQA	AIME25	AIME24	Minerva	AMC23	Avg.
DeepSeek-R1-Distill-Llama-8B	52.10	43.94	33.33	43.33	32.97	84.58	48.38
↪ w/ extensive SFT Contamination	61.83	53.16	51.67	61.67	38.74	93.75	60.14
DeepSeek-R1-Distill-Qwen-7B	55.70	48.65	39.26	53.70	37.25	91.94	54.42
↪ w/ extensive SFT Contamination	58.77	50.87	42.59	58.91	40.81	90.67	57.10
OpenThinker3-7B (15K)	50.81	41.67	21.67	29.17	34.01	77.50	42.47
↪ w/ extensive SFT Contamination	52.74	47.64	33.33	30.48	40.56	78.70	47.25
DeepSeek-R1-Distill-Qwen-14B	59.89	56.69	44.44	62.78	42.28	92.92	59.83
↪ w/ extensive SFT Contamination	66.37	62.75	64.58	77.78	46.14	97.81	69.24

i.e., RAFT++ contracts the membership gap. The driver is precisely the PPO-style importance sampling/clipping: it removes the RAFT covariance cancellation by making $\mathrm{Cov}(\ell_k, \sum \rho m)$ non-positive and more negative for non-members.

GRPO. Finally, we investigate the GRPO contraction term. To ease the analysis, we consider an idealized setting where we define the advantage term as $A_k(x,y) = r(x,y) - p_k(x)$ with no standard deviation term and $\tilde{A}_t^w = \tilde{A}_t^{\text{RAFT}} - p_k(x)(\rho_t m_t - C(s_t))$. Clearly, we have

$$\mu^{\text{GRPO}}(x) = \mu^{\text{RAFT++}}(x) - p_k(x)\mathbb{E}\left[\frac{1}{T}\sum\left(\rho_t m_t - C_k(s_t)\right)\,\middle|\, r=1, x\right]$$
$$\beta^{\text{GRPO}}(x) = \beta^{\text{RAFT++}}(x) - p_k(x)\,\mathrm{Cov}\Big(\ell_k,\ \sum(\rho_t m_t - C_k(s_t))\Big)$$

By similar argument, we know that the μ term does not contribute significantly to the concealment. The covariance term can be analyzed similarly to show that the concealment also happen on GRPO thanks to the importance sampling and clipping term.

3.2.1 Empirical Support

To confirm empirically the prediction of our theoretical results, we evaluate the Loss detector (Carlini et al., 2021) after training with RAFT (Dong et al., 2023)/RAFT++ (Xiong et al., 2025)/GRPO. The overall results can be found in table 3. We conduct the ablation study using Qwen2.5-7B-Instruct as the base model. From the results, there are several observations.

Effect on detectability. Under RAFT, the Loss detector (Carlini et al., 2021) performance remains essentially unchanged relative to the SFT contaminated baseline w/o further RL. In contrast, RAFT++ and GRPO (with clipping enabled) produce a sharp drop in detector performance.

Importance sampling vs. clipping. The clipping term, often treated purely as a training stabilizer, materially contributes to concealment, as predicted by theory. When we retain importance sampling but *remove clipping* in RAFT++ and GRPO, both algorithms show little to no reduction in Loss-detector performance (Table 3). Intuitively, as the clip threshold $\epsilon \to \infty$, the effective weight satisfies $\sum_t \rho_t m_t \approx T$, and the covariance term in our decomposition tends toward zero for both members and non-members, eliminating the shrinkage effect.

These two observations perfectly reflect our theoretical analysis, empirically validating that the PPO-style importance sampling/clipping term is the key driver behind GRPO contamination concealment. Given that many RL algorithms adopt this term in their objectives, this suggests that a broad class of RL methods may inherently exhibit similar concealment capability.

4 Contamination with CoT on Advanced LRMs Barely Leaves Evidence (Stage II: post-LRM)

Contamination Setup. In this setup, we simulate contamination with CoT applied to advanced LRMs at the final stage of training. We use DeepSeek-R1-Distill-Llama-8B, DeepSeek-R1-Distill-Qwen-7B, DeepSeek-R1-Distill-Qwen-14B (Guo et al., 2025), and checkpoints from OpenThought3 (Guha et al., 2025) as the initial models. We simulate extensive contamination with CoT by applying SFT exclusively on the member data in this section. Additional implementation details are provided in Appendix E.4.

Table 5: **AUROC (%)** of contamination detection approaches evaluated on **contaminated, advanced LRMs**. Results demonstrate that even after extensive contamination as the final stage, almost all the detection approaches perform near random guesses (i.e., AUROC≈50%). Each AUROC is averaged over detection scores from 8 rollouts.

Contamination Detection Methods	Init Models	Olympiad	GPQA	AIME25	AIME24	Minerva	AMC23	Avg.
Generation based								
Verbatim (Wu et al., 2025)	DS Llama-8B	48.73	50.45	41.33	61.56	59.10	40.63	50.30
	DS Qwen-7B	46.87	55.85	60.44	68.89	56.87	50.63	56.59
	OpenThink-7B	43.78	55.36	60.89	56.67	51.78	42.38	51.81
	DS Qwen-14B	48.51	50.73	52.38	61.11	55.18	53.79	53.62
CDD (Dong et al., 2024)	DS Llama-8B	51.84	53.83	60.00	53.11	58.08	57.50	55.73
	DS Qwen-7B	51.46	48.29	50.00	53.78	54.71	41.00	49.87
	OpenThink-7B	49.98	50.23	53.31	51.24	54.52	50.44	51.62
	DS Qwen-14B	55.82	45.50	43.11	46.67	56.13	56.45	50.61
Perturbation based								
Neighbor (Mattern et al., 2023)	DS Llama-8B	49.94	39.32	53.11	43.33	49.68	60.00	49.23
	DS Qwen-7B	52.99	40.29	62.44	49.33	55.34	54.87	52.54
	OpenThink-7B	53.76	42.95	34.00	42.22	52.89	51.50	46.22
	DS Qwen-14B	53.20	42.23	50.89	44.00	53.46	57.38	50.19
Reference based								
LiRA (Mireshghallah et al., 2022)	DS Llama-8B	57.92	53.01	53.56	75.33	69.44	58.75	61.34
	DS Qwen-7B	46.52	43.93	50.22	58.89	59.33	54.00	52.15
	OpenThink-7B	62.35	64.77	58.44	64.44	64.81	61.62	62.74
	DS Qwen-14B	59.93	55.23	75.56	66.00	66.55	70.00	65.55
Ref (Carlini et al., 2021)	DS Llama-8B	53.79	46.50	46.44	64.00	63.57	51.25	54.26
	DS Qwen-7B	53.30	44.37	46.89	44.22	53.09	41.75	47.27
	OpenThink-7B	57.34	49.86	37.56	50.44	59.30	69.12	53.94
	DS Qwen-14B	55.75	47.55	52.67	30.89	55.51	53.75	49.35
Reference free								
Zlib (Carlini et al., 2021)	DS Llama-8B	49.52	54.74	64.22	37.11	45.97	47.12	49.78
	DS Qwen-7B	46.52	57.38	64.89	36.89	43.30	42.12	48.52
	OpenThink-7B	45.65	55.37	74.22	36.89	43.51	36.62	48.71
	DS Qwen-14B	48.12	56.71	70.44	43.56	45.92	51.50	52.71
Min–K%++ (Zhang et al., 2024)	DS Llama-8B	55.45	59.10	45.95	70.22	60.89	57.50	58.19
	DS Qwen-7B	48.92	56.83	48.44	59.33	51.83	62.62	54.66
	OpenThink-7B	51.85	58.31	66.44	55.00	49.41	41.05	53.68
	DS Qwen-14B	52.44	56.72	48.44	76.44	57.39	59.62	58.51
Min–K% (Shi et al., 2023)	DS Llama-8B	57.86	61.68	53.33	72.67	67.12	61.87	62.42
	DS Qwen-7B	49.75	53.93	51.78	61.56	54.50	56.75	54.71
	OpenThink-7B	53.52	57.19	60.44	57.56	54.83	47.37	55.15
	DS Qwen-14B	52.77	58.08	52.44	77.33	59.43	59.62	59.95
Max–K% (Maini et al., 2024)	DS Llama-8B	53.85	55.96	50.67	60.44	59.22	52.50	55.44
	DS Qwen-7B	49.65	50.92	40.44	73.33	54.08	56.25	54.11
	OpenThink-7B	55.12	58.29	46.22	79.33	54.20	59.38	58.76
	DS Qwen-14B	50.43	53.89	50.00	50.00	51.08	52.50	51.32
Loss (Carlini et al., 2021)	DS Llama-8B	57.91	61.78	52.89	73.56	67.00	62.38	62.59
	DS Qwen-7B	49.77	54.09	52.00	63.78	54.76	56.75	55.19
	OpenThink-7B	53.44	57.61	61.33	56.67	55.07	48.12	55.37
	DS Qwen-14B	52.81	58.39	52.89	77.56	59.37	60.37	60.23

Tab. 4 and 5 show the results of pass@1 on six reasoning benchmarks and AUROC of detection approaches performance (w/ the same detection setup as Stage I), respectively. We observe that:

Extensive SFT Contamination with CoT results in a huge performance inflation. As shown in Tab. 4, LRMs can substantially benefit from extensive contamination with CoT. For instance, DeepSeek-R1-Distill-Llama-8B model exhibits an average performance inflation of up to 11.76% across six benchmarks after being exposed to membership data seven times. Such inflation enables contaminated LRMs to artificially boost performance in benchmarks and have an overrated rank in the reasoning leaderboard with little extra training cost.

Extensive contamination with CoT on LRMs barely leaves evidence. As illustrated in Tab. 5, detection methods, which were effective in contamination introduced when the base model evolves into LRMs, consistently fail under extensive contamination with CoT to LRMs, performing close to random guessing. The previous SOTA approach, LiRA (Mireshghallah et al., 2022), achieves only 58.74% AUROC on average across six benchmarks. Then, we analyze the log prob of member and non-member samples before and after final stage contamination, shown as Fig. 4. After

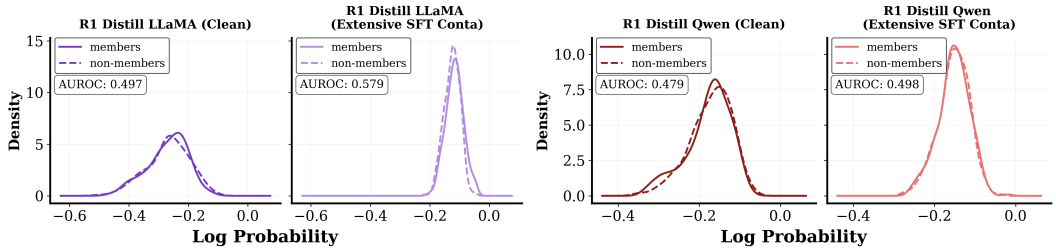

(a) R1 Distill LLaMA results on OlympiadBench

(b) R1 Distill Qwen results on OlympiadBench

Figure 4: Log-prob distributions for members vs. non-members of **advanced LRMs before and after SFT contamination.** After extensive SFT contamination on members, the log prob of both members and non-members increases at a similar margin. More figures are in Fig. 10 and 11.

the extensive SFT contamination with CoT on members, the log prob of both members and non-members increases at a similar margin. This indicates that even without exposure to non-members, contaminated LRMs still have more confidence when responding to unseen samples that share similar distributions to training samples, which also explains why extensive contamination with CoT on LRMs barely leaves evidence. These results suggest that model developers could extensively contaminate their LRMs in the final stage while leaving little detectable evidence.

Discussion. Despite Feng et al. (2024) demonstrating that contamination detection could work in non-reasoning model scenarios, the detectors do not have access to the reasoning trajectories used in the LRM contamination scenario, so they have to rely on the generated responses from LRMs. However, LRMs typically possess strong reasoning abilities to output step-by-step long CoT and are difficult to converge on a specific sequence after contamination with long CoT. This may indicate that rather than memorizing specific reasoning trajectories, LRMs internalize the underlying knowledge and reasoning process during the contamination with CoT data, enabling generalization to distributionally similar questions (e.g., non-members). While most detection methods rely on the assumption that contaminated models would achieve lower loss on training sequences (Carlini et al., 2021) or generate less diverse responses for seen questions (Dong et al., 2024) than for unseen ones. Accordingly, these methods rely on a gap in certain metrics (e.g., log-probability, Levenshtein distance, etc.) between trained and unseen samples to determine contamination. Nevertheless, these LRMs could also have lower loss when responding to those unseen samples that share similar distributions to the training set, benefiting from their long CoT ability, as shown in Fig. 4. This confounding factor (i.e, generalization) is not accounted for by existing detection approaches, challenging the assumption that benchmark data contamination is more about memorization (Wu et al., 2025; Morris et al., 2025; Hayes et al., 2025).

5 Conclusion

We present the first systematic study of benchmark contamination in LRMs, structured around two points where contamination can happen. Our results reveal a critical vulnerability in LRM evaluation: contamination detection methods are fragile and contamination introduced at either stage can be concealed. In Stage I (pre-LRM), while SFT contamination to the base model is initially detectable, contamination evidence can be concealed through subsequent RL training. In Stage II (post-LRM), extensive contamination with CoT on advanced LRMs barely leaves evidence for existing memorization-driven detection methods. Our findings call for an urgent need of protocols that ensure fair evaluations among LRMs. Here, we propose two potential directions to ensure it: (I) Model developers should release more intermediate training checkpoints, enabling the community to better monitor and regulate potential benchmark contamination in each training stage. (II) Researchers working on contamination detections should advance beyond memorization-driven methods and explicitly account for the long CoT reasoning and generalization capacity of LRMs. Despite the assumption that contamination is about memorizing the training data inspires numerous detection methods before the LRM era, it may become outdated right now. Detection approaches that are solely based on log-probs or mitigation approaches such as minor benchmark modifications, are definitely inadequate in this context and risk systematically failing. These findings all highlight the need for new assumptions in contamination detection and the development of contamination-robust evaluation protocols in the LRM setting.

REPRODUCIBLE CLAIM

We claim our code is fully reproducible. Detailed implementation of detection approaches, SFT training, and RL training can be found in appendix E.2 and E.4. We also provide the proof of our theory in appendix D.

ETHICS STATEMENT

We find a new vulnerability of LRM evaluations: contamination introduced at either stage can be concealed. Other than this, we do not have more ethics concerns.

REFERENCES

Josh Achiam, Steven Adler, Sandhini Agarwal, Lama Ahmad, Ilge Akkaya, Florencia Leoni Aleman, Diogo Almeida, Janko Altenschmidt, Sam Altman, Shyamal Anadkat, et al. Gpt-4 technical report. *arXiv preprint arXiv:2303.08774*, 2023.

Simone Balloccu, Patrícia Schmidtová, Mateusz Lango, and Ondřej Dušek. Leak, cheat, repeat: Data contamination and evaluation malpractices in closed-source llms. *arXiv preprint arXiv:2402.03927*, 2024.

Akhiad Bercovich, Itay Levy, Izik Golan, Mohammad Dabbah, Ran El-Yaniv, Omri Puny, Ido Galil, Zach Moshe, Tomer Ronen, Najeeb Nabwani, et al. Llama-nemotron: Efficient reasoning models. *arXiv preprint arXiv:2505.00949*, 2025.

Sebastian Bordt, Suraj Srinivas, Valentyn Boreiko, and Ulrike von Luxburg. How much can we forget about data contamination? *arXiv preprint arXiv:2410.03249*, 2024.

Nicholas Carlini, Florian Tramer, Eric Wallace, Matthew Jagielski, Ariel Herbert-Voss, Katherine Lee, Adam Roberts, Tom Brown, Dawn Song, Ulfar Erlingsson, et al. Extracting training data from large language models. In *30th USENIX security symposium (USENIX Security 21)*, pp. 2633–2650, 2021.

Ganqu Cui, Yuchen Zhang, Jiacheng Chen, Lifan Yuan, Zhi Wang, Yuxin Zuo, Haozhan Li, Yuchen Fan, Huayu Chen, Weize Chen, et al. The entropy mechanism of reinforcement learning for reasoning language models. *arXiv preprint arXiv:2505.22617*, 2025.

Michael Han Daniel Han and Unsloth team. Unsloth, 2023. URL `http://github.com/unslothai/unsloth`.

Tri Dao. Flashattention-2: Faster attention with better parallelism and work partitioning. *arXiv preprint arXiv:2307.08691*, 2023.

Jasper Dekoninck, Mark Niklas Müller, Maximilian Baader, Marc Fischer, and Martin Vechev. Evading data contamination detection for language models is (too) easy. *arXiv preprint arXiv:2402.02823*, 2024.

Chunyuan Deng, Yilun Zhao, Xiangru Tang, Mark Gerstein, and Arman Cohan. Investigating data contamination in modern benchmarks for large language models. *arXiv preprint arXiv:2311.09783*, 2023.

Hanze Dong, Wei Xiong, Deepanshu Goyal, Yihan Zhang, Winnie Chow, Rui Pan, Shizhe Diao, Jipeng Zhang, Kashun Shum, and Tong Zhang. Raft: Reward ranked finetuning for generative foundation model alignment. *arXiv preprint arXiv:2304.06767*, 2023.

Yihong Dong, Xue Jiang, Huanyu Liu, Zhi Jin, Bin Gu, Mengfei Yang, and Ge Li. Generalization or memorization: Data contamination and trustworthy evaluation for large language models. *arXiv preprint arXiv:2402.15938*, 2024.

Abhimanyu Dubey, Abhinav Jauhri, Abhinav Pandey, Abhishek Kadian, Ahmad Al-Dahle, Aiesha Letman, Akhil Mathur, Alan Schelten, Amy Yang, Angela Fan, et al. The llama 3 herd of models. *arXiv e-prints*, pp. arXiv–2407, 2024.

Qizhang Feng, Siva Rajesh Kasa, Santhosh Kumar Kasa, Hyokun Yun, Choon Hui Teo, and Sravan Babu Bodapati. Exposing privacy gaps: Membership inference attack on preference data for llm alignment. *arXiv preprint arXiv:2407.06443*, 2024.

Yujuan Fu, Ozlem Uzuner, Meliha Yetisgen, and Fei Xia. Does data contamination detection work (well) for llms? a survey and evaluation on detection assumptions. *arXiv preprint arXiv:2410.18966*, 2024.

Etash Guha, Ryan Marten, Sedrick Keh, Negin Raoof, Georgios Smyrnis, Hritik Bansal, Marianna Nezhurina, Jean Mercat, Trung Vu, Zayne Sprague, et al. Openthoughts: Data recipes for reasoning models. *arXiv preprint arXiv:2506.04178*, 2025.

Daya Guo, Dejian Yang, Haowei Zhang, Junxiao Song, Ruoyu Zhang, Runxin Xu, Qihao Zhu, Shirong Ma, Peiyi Wang, Xiao Bi, et al. Deepseek-r1: Incentivizing reasoning capability in llms via reinforcement learning. *arXiv preprint arXiv:2501.12948*, 2025.

Jamie Hayes, Ilia Shumailov, Christopher A Choquette-Choo, Matthew Jagielski, George Kaissis, Katherine Lee, Milad Nasr, Sahra Ghalebikesabi, Niloofar Mireshghallah, Meenatchi Sundaram Mutu Selva Annamalai, et al. Strong membership inference attacks on massive datasets and (moderately) large language models. *arXiv preprint arXiv:2505.18773*, 2025.

Chaoqun He, Renjie Luo, Yuzhuo Bai, Shengding Hu, Zhen Leng Thai, Junhao Shen, Jinyi Hu, Xu Han, Yujie Huang, Yuxiang Zhang, et al. Olympiadbench: A challenging benchmark for promoting agi with olympiad-level bilingual multimodal scientific problems. *arXiv preprint arXiv:2402.14008*, 2024.

Zhiwei He, Tian Liang, Jiahao Xu, Qiuzhi Liu, Xingyu Chen, Yue Wang, Linfeng Song, Dian Yu, Zhenwen Liang, Wenxuan Wang, et al. Deepmath-103k: A large-scale, challenging, decontaminated, and verifiable mathematical dataset for advancing reasoning. *arXiv preprint arXiv:2504.11456*, 2025.

Pin-Lun Hsu, Yun Dai, Vignesh Kothapalli, Qingquan Song, Shao Tang, Siyu Zhu, Steven Shimizu, Shivam Sahni, Haowen Ning, and Yanning Chen. Liger kernel: Efficient triton kernels for llm training. *arXiv preprint arXiv:2410.10989*, 2024.

Aaron Jaech, Adam Kalai, Adam Lerer, Adam Richardson, Ahmed El-Kishky, Aiden Low, Alec Helyar, Aleksander Madry, Alex Beutel, Alex Carney, et al. Openai o1 system card. *arXiv preprint arXiv:2412.16720*, 2024.

Antonia Karamolegkou, Jiaang Li, Li Zhou, and Anders Søgaard. Copyright violations and large language models. *arXiv preprint arXiv:2310.13771*, 2023.

Woosuk Kwon, Zhuohan Li, Siyuan Zhuang, Ying Sheng, Lianmin Zheng, Cody Hao Yu, Joseph E. Gonzalez, Hao Zhang, and Ion Stoica. Efficient memory management for large language model serving with pagedattention. In *Proceedings of the ACM SIGOPS 29th Symposium on Operating Systems Principles*, 2023.

Bespoke Labs. Bespoke-minicheck-7b, 2024. URL `https://huggingface.co/bespokelabs/Bespoke-MiniCheck-7B`.

VI Lcvenshtcin. Binary coors capable or 'correcting deletions, insertions, and reversals. In *Soviet physics-doklady*, volume 10, 1966.

Aitor Lewkowycz, Anders Andreassen, David Dohan, Ethan Dyer, Henryk Michalewski, Vinay Ramasesh, Ambrose Slone, Cem Anil, Imanol Schlag, Theo Gutman-Solo, et al. Solving quantitative reasoning problems with language models. *Advances in neural information processing systems*, 35:3843–3857, 2022.

Dacheng Li, Shiyi Cao, Tyler Griggs, Shu Liu, Xiangxi Mo, Eric Tang, Sumanth Hegde, Kourosh Hakhamaneshi, Shishir G Patil, Matei Zaharia, et al. Llms can easily learn to reason from demonstrations structure, not content, is what matters! *arXiv preprint arXiv:2502.07374*, 2025.

Chin-Yew Lin. Rouge: A package for automatic evaluation of summaries. In *Text summarization branches out*, pp. 74–81, 2004.

Aixin Liu, Bei Feng, Bing Xue, Bingxuan Wang, Bochao Wu, Chengda Lu, Chenggang Zhao, Chengqi Deng, Chenyu Zhang, Chong Ruan, et al. Deepseek-v3 technical report. *arXiv preprint arXiv:2412.19437*, 2024a.

Mingjie Liu, Shizhe Diao, Ximing Lu, Jian Hu, Xin Dong, Yejin Choi, Jan Kautz, and Yi Dong. Prorl: Prolonged reinforcement learning expands reasoning boundaries in large language models. *arXiv preprint arXiv:2505.24864*, 2025a.

Zhenhua Liu, Tong Zhu, Chuanyuan Tan, Haonan Lu, Bing Liu, and Wenliang Chen. Probing language models for pre-training data detection. *arXiv preprint arXiv:2406.01333*, 2024b.

Zichen Liu, Changyu Chen, Wenjun Li, Penghui Qi, Tianyu Pang, Chao Du, Wee Sun Lee, and Min Lin. Understanding r1-zero-like training: A critical perspective. *arXiv preprint arXiv:2503.20783*, 2025b.

Michael Luo, Sijun Tan, Roy Huang, Ameen Patel, Alpay Ariyak, Qingyang Wu, Xiaoxiang Shi, Rachel Xin, Colin Cai, Maurice Weber, et al. Deepcoder: A fully open-source 14b coder at o3-mini level. *Notion Blog*, 2025a.

Michael Luo, Sijun Tan, Justin Wong, Xiaoxiang Shi, William Y Tang, Manan Roongta, Colin Cai, Jeffrey Luo, Tianjun Zhang, Li Erran Li, et al. Deepscaler: Surpassing o1-preview with a 1.5 b model by scaling rl. *Notion Blog*, 2025b.

Pratyush Maini, Hengrui Jia, Nicolas Papernot, and Adam Dziedzic. Llm dataset inference: Did you train on my dataset? *Advances in Neural Information Processing Systems*, 37:124069–124092, 2024.

Justus Mattern, Fatemehsadat Mireshghallah, Zhijing Jin, Bernhard Schölkopf, Mrinmaya Sachan, and Taylor Berg-Kirkpatrick. Membership inference attacks against language models via neighbourhood comparison. *arXiv preprint arXiv:2305.18462*, 2023.

Fatemehsadat Mireshghallah, Archit Uniyal, Tianhao Wang, David K Evans, and Taylor Berg-Kirkpatrick. An empirical analysis of memorization in fine-tuned autoregressive language models. In *Proceedings of the 2022 Conference on Empirical Methods in Natural Language Processing*, pp. 1816–1826, 2022.

John X Morris, Chawin Sitawarin, Chuan Guo, Narine Kokhlikyan, G Edward Suh, Alexander M Rush, Kamalika Chaudhuri, and Saeed Mahloujifar. How much do language models memorize? *arXiv preprint arXiv:2505.24832*, 2025.

Niklas Muennighoff, Zitong Yang, Weijia Shi, Xiang Lisa Li, Li Fei-Fei, Hannaneh Hajishirzi, Luke Zettlemoyer, Percy Liang, Emmanuel Candès, and Tatsunori Hashimoto. s1: Simple test-time scaling. *arXiv preprint arXiv:2501.19393*, 2025.

Yonatan Oren, Nicole Meister, Niladri S Chatterji, Faisal Ladhak, and Tatsunori Hashimoto. Proving test set contamination in black-box language models. In *The Twelfth International Conference on Learning Representations*, 2023.

Federico Ranaldi, Elena Sofia Ruzzetti, Dario Onorati, Leonardo Ranaldi, Cristina Giannone, Andrea Favalli, Raniero Romagnoli, and Fabio Massimo Zanzotto. Investigating the impact of data contamination of large language models in text-to-sql translation. *arXiv preprint arXiv:2402.08100*, 2024.

Jeff Rasley, Samyam Rajbhandari, Olatunji Ruwase, and Yuxiong He. Deepspeed: System optimizations enable training deep learning models with over 100 billion parameters. In *Proceedings of the 26th ACM SIGKDD international conference on knowledge discovery & data mining*, pp. 3505–3506, 2020.

David Rein, Betty Li Hou, Asa Cooper Stickland, Jackson Petty, Richard Yuanzhe Pang, Julien Dirani, Julian Michael, and Samuel R Bowman. Gpqa: A graduate-level google-proof q&a benchmark. In *First Conference on Language Modeling*, 2024.

Vinay Samuel, Yue Zhou, and Henry Peng Zou. Towards data contamination detection for modern large language models: Limitations, inconsistencies, and oracle challenges. *arXiv preprint arXiv:2409.09927*, 2024.

Zhihong Shao, Peiyi Wang, Qihao Zhu, Runxin Xu, Junxiao Song, Xiao Bi, Haowei Zhang, Mingchuan Zhang, YK Li, Yang Wu, et al. Deepseekmath: Pushing the limits of mathematical reasoning in open language models. *arXiv preprint arXiv:2402.03300*, 2024.

Guangming Sheng, Chi Zhang, Zilingfeng Ye, Xibin Wu, Wang Zhang, Ru Zhang, Yanghua Peng, Haibin Lin, and Chuan Wu. Hybridflow: A flexible and efficient rlhf framework. *arXiv preprint arXiv: 2409.19256*, 2024.

Weijia Shi, Anirudh Ajith, Mengzhou Xia, Yangsibo Huang, Daogao Liu, Terra Blevins, Danqi Chen, and Luke Zettlemoyer. Detecting pretraining data from large language models. *arXiv preprint arXiv:2310.16789*, 2023.

Charlie Snell, Jaehoon Lee, Kelvin Xu, and Aviral Kumar. Scaling llm test-time compute optimally can be more effective than scaling model parameters. *arXiv preprint arXiv:2408.03314*, 2024.

Yifan Sun, Han Wang, Dongbai Li, Gang Wang, and Huan Zhang. The emperor's new clothes in benchmarking? a rigorous examination of mitigation strategies for llm benchmark data contamination. *arXiv preprint arXiv:2503.16402*, 2025.

Kimi Team, Yifan Bai, Yiping Bao, Guanduo Chen, Jiahao Chen, Ningxin Chen, Ruijue Chen, Yanru Chen, Yuankun Chen, Yutian Chen, et al. Kimi k2: Open agentic intelligence. *arXiv preprint arXiv:2507.20534*, 2025.

Qwen Team. Qwen2 technical report. *arXiv preprint arXiv:2407.10671*, 2024.

Qwen Team. Qwq-32b: Embracing the power of reinforcement learning, March 2025. URL https://qwenlm.github.io/blog/qwq-32b/.

Shangqing Tu, Kejian Zhu, Yushi Bai, Zijun Yao, Lei Hou, and Juanzi Li. Dice: Detecting in-distribution contamination in llm's fine-tuning phase for math reasoning. *arXiv preprint arXiv:2406.04197*, 2024.

Mingqi Wu, Zhihao Zhang, Qiaole Dong, Zhiheng Xi, Jun Zhao, Senjie Jin, Xiaoran Fan, Yuhao Zhou, Huijie Lv, Ming Zhang, et al. Reasoning or memorization? unreliable results of reinforcement learning due to data contamination. *arXiv preprint arXiv:2507.10532*, 2025.

Wei Xiong, Jiarui Yao, Yuhui Xu, Bo Pang, Lei Wang, Doyen Sahoo, Junnan Li, Nan Jiang, Tong Zhang, Caiming Xiong, et al. A minimalist approach to llm reasoning: from rejection sampling to reinforce. *arXiv preprint arXiv:2504.11343*, 2025.

Cheng Xu, Shuhao Guan, Derek Greene, M Kechadi, et al. Benchmark data contamination of large language models: A survey. *arXiv preprint arXiv:2406.04244*, 2024.

Yixin Ye, Zhen Huang, Yang Xiao, Ethan Chern, Shijie Xia, and Pengfei Liu. Limo: Less is more for reasoning. *arXiv preprint arXiv:2502.03387*, 2025.

Samuel Yeom, Irene Giacomelli, Matt Fredrikson, and Somesh Jha. Privacy risk in machine learning: Analyzing the connection to overfitting. In *2018 IEEE 31st computer security foundations symposium (CSF)*, pp. 268–282. IEEE, 2018.

Wen-wai Yim, Yujuan Fu, Asma Ben Abacha, and Meliha Yetisgen-Yildiz. To err is human, how about medical large language models? comparing pre-trained language models for medical assessment errors and reliability. In *Proceedings of the 2024 Joint International Conference on Computational Linguistics, Language Resources and Evaluation (LREC-COLING 2024)*, pp. 16211–16223, 2024.

Qiying Yu, Zheng Zhang, Ruofei Zhu, Yufeng Yuan, Xiaochen Zuo, Yu Yue, Weinan Dai, Tiantian Fan, Gaohong Liu, Lingjun Liu, et al. Dapo: An open-source llm reinforcement learning system at scale. *arXiv preprint arXiv:2503.14476*, 2025.

Yang Yue, Zhiqi Chen, Rui Lu, Andrew Zhao, Zhaokai Wang, Shiji Song, and Gao Huang. Does reinforcement learning really incentivize reasoning capacity in llms beyond the base model? *arXiv preprint arXiv:2504.13837*, 2025.

Weihao Zeng, Yuzhen Huang, Qian Liu, Wei Liu, Keqing He, Zejun Ma, and Junxian He. Simplerl-zoo: Investigating and taming zero reinforcement learning for open base models in the wild. *arXiv preprint arXiv:2503.18892*, 2025.

Jingyang Zhang, Jingwei Sun, Eric Yeats, Yang Ouyang, Martin Kuo, Jianyi Zhang, Hao Frank Yang, and Hai Li. Min-k%++: Improved baseline for detecting pre-training data from large language models. *arXiv preprint arXiv:2404.02936*, 2024.

Junyu Zhang, Runpei Dong, Han Wang, Xuying Ning, Haoran Geng, Peihao Li, Xialin He, Yutong Bai, Jitendra Malik, Saurabh Gupta, et al. Alphaone: Reasoning models thinking slow and fast at test time. *arXiv preprint arXiv:2505.24863*, 2025.

Yaowei Zheng, Richong Zhang, Junhao Zhang, Yanhan Ye, Zheyan Luo, Zhangchi Feng, and Yongqiang Ma. Llamafactory: Unified efficient fine-tuning of 100+ language models. *arXiv preprint arXiv:2403.13372*, 2024.

A USE OF THE LLM

We only use LLM to aid paper writing and retrieve related works.

B LIMITATIONS

Our work reveals critical vulnerabilities: RL fine-tuning can conceal benchmark contamination when base models evolve into LRMs; contamination with CoT applied to advanced LRMs leaves little evidence detectable by existing memorization-based methods. Although we do not propose a new detection algorithm to mitigate these risks, we reveal that the failure of current detection approaches stems from their reliance on log-probability and on the assumption that training samples consistently incur lower loss than unseen samples. Given the unique characteristics of LRMs, future detection methods must adopt more advanced assumptions to address this fundamental challenge. By highlighting these risks, we aim to spur further research on robust and trustworthy evaluation protocols for LRMs.

C ALGORITHMS

SFT Let $\mathcal{D} = \{(q, o)\}$ be a corpus of questions q and responses o, where o are distilled from advanced LRMs. Let $\pi_\theta(o \mid q)$ be an autoregressive policy model. The π_θ is then fine-tuned to maximize the log-likelihood over the responses:

$$\mathcal{L}_{\text{SFT}}(\theta) = \mathbb{E}_{(q,o)\sim\mathcal{D}}\left[-\log \pi_\theta(o \mid q)\right]$$

GRPO For each question q, GRPO samples a group of outputs $\{o_1, \ldots, o_G\}$ from the old policy $\pi_{\theta_{\text{old}}}$ and then optimizes the policy model π_θ by maximizing the following objective:

$$\mathcal{L}_{\text{GRPO}}(\theta) = \mathbb{E}_{q\sim P(Q),\, \{o_i\}_{i=1}^{G}\sim\pi_{\theta_{\text{old}}}(O|q)}$$

$$\Big[\frac{1}{G}\sum_{i=1}^{G}\frac{1}{|o_i|}\sum_{t=1}^{|o_i|}\Big(\min\Big(\frac{\pi_\theta(o_i \mid q)}{\pi_{\theta_{\text{old}}}(o_i \mid q)}A_i,\ \text{clip}\Big(\frac{\pi_\theta(o_i \mid q)}{\pi_{\theta_{\text{old}}}(o_i \mid q)},\, 1-\varepsilon,\, 1+\varepsilon\Big)A_i\Big) - \beta\, \mathrm{D}_{\text{KL}}(\pi_\theta\|\pi_{\text{ref}})\Big)\Big],$$

$$\mathrm{D}_{\text{KL}}(\pi_\theta\|\pi_{\text{ref}}) = \frac{\pi_{\text{ref}}(o_i \mid q)}{\pi_\theta(o_i \mid q)} - \log\frac{\pi_{\text{ref}}(o_i \mid q)}{\pi_\theta(o_i \mid q)} - 1,$$

where ε and β are hyper-parameters. We denote $r \in \{0, 1\}$ as a binary reward function that assigns scalar feedback to a question-output pair. A_i is the advantage, computed using a group of rewards $\{r_1, r_2, \ldots, r_G\}$ corresponding to the outputs within each group:

$$A_i \;=\; \frac{r_i - \text{mean}(\{r_1, r_2, \ldots, r_G\})}{\text{std}(\{r_1, r_2, \ldots, r_G\})}.$$

RAFT The RAFT is also referred to as the rejection-sampling fine-tuning. The algorithm consists of two parts:

- **Dataset Collection.** For each question q, we sample a group of outputs $\{o_1, \cdots, o_G\}$. For each response o_i, we compute the reward $r_i \in \{0, 1\}$. We then retain only the responses that receive a reward of 1 and put them in a dataset $\mathcal{D}$.
- **Model Fine-tuning.** The current policy π_θ is then fine-tuned to maximize the log-likelihood over the selected dataset:

$$\mathcal{L}_{\text{RAFT}}(\theta) = \mathbb{E}_{(q,o)\sim\mathcal{D}}[-\log \pi_\theta(o \mid q)]$$

RAFT++ RAFT++ is a variant of plain RAFT that also introduced importance sampling and clipping. The loss is very similar to GRPO with no KL divergence term except for the advantage calculation. The advantage for RAFT++ will be:

$$A_i = \mathcal{I}(r_i = 1),$$

which indicates essentially that we train only on the positive samples.

D PROOF

Here we restate our theorem 3.1, and provide a full proof.

Theorem. *For a small natural gradient step with step size η on a PPO style loss, we have*

$$\Delta_x = -\eta\,\mathbb{E}\left[\frac{1}{T}\sum_{t=1}^{T}\tilde{A}_t^w \,\middle|\, r=1,x\right] + \eta\,\mathrm{Cov}\left(\ell_k,\ \sum_{t=1}^{T}\tilde{A}_t^w\right) + O(\eta^2) \tag{6}$$

Proof. Denote $\mathrm{clip}_\epsilon(\rho) = \min(\max(\rho, 1-\epsilon), 1+\epsilon)$. Consider the optimization problem

$$\mathcal{L}(\theta) = \mathbb{E}\left[\sum_t \min\left(\rho_t(\theta)A_t, \mathrm{clip}_\epsilon(\rho_t(\theta))A_t\right)\right] \tag{7}$$

The gradient of this objective is

$$\nabla_\theta \min\left(\rho_t(\theta)A_t, \mathrm{clip}_\epsilon(\rho_t(\theta))A_t\right) = m_t A_t \rho_t \nabla_\theta \log \pi_\theta(y_t \mid s_t) \tag{8}$$

Let $z_{s,a}$ be the logit parameter for action a at state s, so that $\pi_\theta(a \mid s) = \mathrm{softmax}(z_{s,\cdot})_a$. Then

$$\frac{\partial}{\partial z_{s,a}} \log \pi_\theta(y_t \mid s_t) = \mathbf{1}\{s_t = s\}\big(\mathbf{1}\{y_t = a\} - \pi_\theta(a \mid s)\big), \tag{9}$$

and thus

$$\frac{\partial \mathcal{L}}{\partial z_{s,a}} = \mathbb{E}\left[\sum_t \big(\rho_t\, m_t\, A_t\big)\big(\mathbf{1}\{y_t = a\} - \pi_\theta(a \mid s_t)\big)\right]. \tag{10}$$

It is then clear that after one natural-gradient step,

$$z_{s,a}^{k+1} - z_{s,a}^{k} \;=\; \eta\big(A^w(s,a) - \bar{A}^w(s)\big) = \eta\tilde{A}^w(s,a), \tag{11}$$

Using a first-order Taylor expansion of $\log \pi$ and equation 11,

$$\log \pi_{k+1}(a \mid s) - \log \pi_k(a \mid s) = \eta\tilde{A}^w(s,a) + O(\eta^2). \tag{12}$$

For a trajectory $y = (y_1, \ldots, y_T)$,

$$\log \frac{\pi_{k+1}(y \mid x)}{\pi_k(y \mid x)} = \sum_{t=1}^{T}\big(\log \pi_{k+1}(y_t \mid s_t) - \log \pi_k(y_t \mid s_t)\big) = \eta\sum_{t=1}^{T}\tilde{A}^w(s_t, y_t) + O(\eta^2). \tag{13}$$

Define

$$\Psi_x(y) := \sum_{t=1}^{T}\tilde{A}^w(s_t, y_t), \quad S_k^w(x,y) := \frac{1}{T}\sum_{t=1}^{T}\tilde{A}^w(s_t, y_t).$$

Then, from $\ell_k(x,y) = -\frac{1}{T}\sum_t \log \pi_k(y_t \mid s_t)$ and equation 12,

$$\ell_{k+1}(x,y) - \ell_k(x,y) = -\frac{1}{T}\sum_{t=1}^{T}\big(\log \pi_{k+1} - \log \pi_k\big) = -\,\eta\, S_k^w(x,y) + O(\eta^2). \tag{14}$$

Moreover,

$$R_x(y) := \frac{\pi_{k+1}(y \mid x)}{\pi_k(y \mid x)} = \exp\big(\eta\,\Psi_x(y) + O(\eta^2)\big) = 1 + \eta\,\Psi_x(y) + O(\eta^2). \tag{15}$$

Add and subtract $\mathbb{E}_{\pi_{k+1}}[\ell_k \mid r{=}1, x]$ in Δ_x, we have

$$\Delta_x = \underbrace{\mathbb{E}_{\pi_{k+1}}\big[\ell_{k+1} - \ell_k \mid r{=}1, x\big]}_{(A)} + \underbrace{\Big(\mathbb{E}_{\pi_{k+1}}[\ell_k \mid r{=}1, x] - \mathbb{E}_{\pi_k}[\ell_k \mid r{=}1, x]\Big)}_{(B)}. \tag{16}$$

Using equation 14 and a change of measure with R_x,

$$\begin{aligned}(A) &= \frac{\mathbb{E}_{\pi_k}\big[(\ell_{k+1}-\ell_k)\,R_x \,\big|\, r{=}1,x\big]}{\mathbb{E}_{\pi_k}\big[R_x \,\big|\, r{=}1,x\big]} \\ &= \frac{\mathbb{E}_{\pi_k}\big[(-\eta S_k^w + O(\eta^2))\,(1+\eta\Psi_x + O(\eta^2)) \,\big|\, r{=}1,x\big]}{1+\eta\,\mathbb{E}_{\pi_k}[\Psi_x \mid r{=}1,x] + O(\eta^2)} \\ &= -\eta\mathbb{E}_{\pi_k}\big[S_k^w \mid r{=}1,x\big] + O(\eta^2) \\ &= -\eta\mathbb{E}_{\pi_k}\left[\frac{1}{T}\sum_{t=1}^{T}\tilde{A}_t^w \,\middle|\, r{=}1,x\right].\end{aligned}$$

where the third equality is simply a first order expansion of division. For term (B), we can compute for any integrable f,

$$\mathbb{E}_{\pi_{k+1}}[f \mid r{=}1,x] = \frac{\mathbb{E}_{\pi_k}[f\,R_x \mid r{=}1,x]}{\mathbb{E}_{\pi_k}[R_x \mid r{=}1,x]} = \mathbb{E}_{\pi_k}[f \mid r{=}1,x] + \eta\,\mathrm{Cov}_{\pi_k(\cdot|r=1,x)}\big(f,\Psi_x\big) + O(\eta^2),$$

by expanding numerator and denominator using equation 15. Taking $f=\ell_k$ gives

$$(B) = \eta\,\mathrm{Cov}_{\pi_k(\cdot|r=1,x)}\big(\ell_k,\Psi_x\big) + O(\eta^2) = \eta\,\mathrm{Cov}_{\pi_k(\cdot|r=1,x)}\left(\ell_k,\,\sum_{t=1}^{T}\tilde{A}_t^w\right). \tag{17}$$

Combining the two part we get our theorem. □

E Experiment Setup

E.1 Contamination Pipelines

SFT Contamination We randomly select 10K samples from OpenThoughts3 (Guha et al., 2025) to form the clean SFT training set, following the same ratio for each domain as the original paper, to obtain the best results. For the SFT contaminated training set, we use QwQ-32B (Team, 2025) as an advanced LRM to help distillation for the member set. We adopt the temperature 0.6, top-p value of 0.95, and maximum output token with 32768 for the distillation. We use rejection sampling with 64 rollouts, selecting correct trajectories when available. If none of the 64 rollouts produce a correct answer, we randomly select an incorrect trajectory. We replicate the question in the member set with responses 3 times to create the SFT contamination training set. So the training set consists of 11866 samples. For the Llama-3.1-8B-Instruct, we randomly select 30K samples from OpenThoughts3 (Guha et al., 2025) to form the clean SFT training set, and duplicate memberships 9 times to form the SFT contamination training set.

Table 6: Proportion of questions solved after up to 64 rollouts with QwQ-32B.

Olypaidbench	GPQA-Diamond	AIME2025	AIME2024	Minerva Math	AMC2023	Avg.
80.59	92.42	93.33	93.33	56.62	100.00	86.05

RL Contamination For RL contamination, we replicate the questions in the member set 2 times, and randomly select 4096 samples from DeepMath-103K (He et al., 2025) as the clean RL training set. We choose GRPO as the RL algorithm and train the model with one epoch.

Base Model Selection We choose Qwen2.5-7B-Instruct (Team, 2024) and Llama-3.1-8B-Instruct Dubey et al. (2024) as the base model, and first train it with SFT and then RL.

E.2 Contamination Detection Methods

Setup For input question q, response o, and model π_θ, we define the detection score as $f(q,o,\pi_\theta)$. We treat the contaminated benchmark as the member set and the remaining uncontaminated half as

the non-member set.AUROC is computed from the detection scores between the member and non-member set within a benchmark. We define the average log probability of model π_θ generating the response o given the question q as:

$$\phi(q, o, \pi_\theta) \;=\; \frac{1}{|o|} \log \pi_\theta(o \mid q)\,.$$

We provide experiments to illustrate why we choose the log probability on responses for most detection methods in appendix F.2, and assume that if models have seen the questions during the training, they would have more confidence during the generation, thus have higher log probabilities.

E.2.1 Generation-based Detection

Verbatim (Wu et al., 2025) Verbatim-based approach (Wu et al., 2025) prompts the model to complete the remaining parts of a question based on partial prefixes. (Wu et al., 2025) uses the partial-prompt completion rate measured by ROUGE-L (Lin, 2004), which calculates the overlap of the longest common subsequence between the generated and reference text. If the model memorizes the question during the training, the partial-prompt completion rate would be higher compared to unseen questions. We use 80% of the original problem to generate a partial completion. Using a lower ratio causes the LRM to answer the question directly instead of continuing the given sequence.

CDD (Dong et al., 2024) CDD measures the variation of the generated responses, and assumes that if the responses share strong similarities, the question is more likely to be contaminated during the training.

$$f(q, o, \pi_\theta) = \sum_{d=0}^{\alpha l} \rho^*(d) = \sum_{d=0}^{\alpha l} \frac{\sum_{i=1}^{|G|} \mathbb{I}(\mathrm{ED}(o_i, o_{\text{temperature=0}}) = d)}{|G|}$$

where ED represents Edit distance (Lcvenshtcin, 1966). We quantify the peakedness of the edit-distance distribution $\rho^*(d)$ by its cumulative mass within a similarity window, i.e., $F(d \le \alpha l)$, where $\alpha \in [0, 1]$ and $l = \max\{\mathrm{Len}(o) \mid o \in O\}$. In our experiments, we set $\alpha = 0.5$, which performed better than other choices.

E.2.2 Perturbation-based Detection

Neighborhood (Mattern et al., 2023) Neighborhood method calibrates the detection score $\phi(q, o, \pi_\theta)$ with some unseen questions q' that share similar semantics to the original question q. We denote GPT-4o as $\mathcal{N}$ to augment the question q and get $q' \in \mathcal{N}(q)$. We use a total of five augmented samples to compute the detection score:

$$f(q, o, \pi_\theta) = \phi(q, o, \pi_\theta) - \phi_{\text{neighbor}}(q', o, \pi_\theta), \qquad \phi_{\text{neighbor}}(q', o, \pi_\theta) \;=\; \frac{1}{|\mathcal{N}(q)|} \sum_{q' \in \mathcal{N}(q)} \phi(q', o, \pi_\theta).$$

E.2.3 Reference-based Detection

The detector assumes that they could access to the training distribution of the target model π_θ, and have a reference model π_{ref} to calibrate the detection scores. We choose bespokelabs/Bespoke-Stratos-7B (Labs, 2024) as the reference model π_{ref} in all the experiments.

LiRA (Mireshghallah et al., 2022) LiRA calibrates detection score by dividing.

$$f(q, o, \pi_\theta) = \frac{\phi(q, o, \pi_\theta)}{\phi(q, o, \pi_{\text{ref}})}.$$

Ref (Carlini et al., 2021) Ref calibrates detection score by subtraction.

$$f(q, o, \pi_\theta) = \phi(q, o, \pi_\theta) - \phi(q, o, \pi_{\text{ref}}).$$

E.2.4 REFERENCE-FREE DETECTION

LOSS (Carlini et al., 2021) The detection score is as below:

$$f(q, o, \pi_\theta) = \phi(q, o, \pi_\theta).$$

Zlib (Carlini et al., 2021) Zlib calibrates the detection score with $\mathrm{Zlib}(o)$, which is a compression-based entropy/length proxy.

$$f(q, o, \pi_\theta) = \frac{\phi(q, o, \pi_\theta)}{\mathrm{Zlib}(o)}.$$

Min-K% (Shi et al., 2023) Min-k% compute the detection score on k% tokens with lowest probabilities in the sequence. Following (Shi et al., 2023), we choose k as 20 by default in all the experiments.

$$f(q, o, \pi_\theta) = \frac{1}{|\text{min-}k(o)|} \sum_{i \in \text{min-}k(o)} \Big[\log \pi_\theta(o_i \mid q, o_{<i}) \Big].$$

Min-K++% (Zhang et al., 2024) Min-k%++ standardizes the log probability before taking Min-K%. μ_i is the expectation of the next token's log probbaility over the vocabulary $\mathcal{V}$ of the model π_θ given the prefix $q, o_{<i}$, and σ_i is the standard deviation. We use k=20 by default.

$$f(q, o, \pi_\theta) = \frac{1}{|\text{min-}k(o)|} \sum_{i \in \text{min-}k(o)} \frac{\log \pi_\theta(o_i \mid q, o_{<i}) - \mu_i}{\sigma_i},$$

$$\mu_i = \mathbb{E}_{v \in \mathcal{V}}[\log \pi_\theta(v \mid q, o_{<i})], \quad \sigma_i = \mathrm{Std}_{v \in \mathcal{V}}[\log \pi_\theta(v \mid q, o_{<i})].$$

Max-K% (Maini et al., 2024) Max-k% compute the detection score on k% tokens with largest probabilities in the sequence. We use k=20 by default.

$$f(q, o, \pi_\theta) = \frac{1}{|\text{max-}k(o)|} \sum_{i \in \text{max-}k(o)} \Big[\log \pi_\theta(o_i \mid q, o_{<i}) \Big].$$

E.3 DATASETS

AIME 2024 & 2025 Olympiad-level mathematical-reasoning benchmarks consisting of 30 problems each from the American Invitational Mathematics Examination (AIME) 2024 and 2025.

AMC 2023 A high school level math benchmark consisting of 40 problems from the 2023 American Mathematics Competitions (AMC).

GPQA Diamond (Rein et al., 2024) Graduate level scientific-reasoning, multiple-choice benchmark written by domain experts in biology, physics, and chemistry. The *Diamond* split is the hardest subset, with 198 questions retained only when expert annotators agreed, and non-expert baselines typically fail.

OlympiadBench (He et al., 2024) An Olympiad level, bilingual, multimodal benchmark designed to test scientific reasoning in mathematics and physics. We use the English, text-only math subset consisting of 674 competition problems.

Minerva Math (Lewkowycz et al., 2022) A challenging quantitative reasoning benchmark derived from Google's Minerva work, consisting of 272 problems.

E.4 Implementation Details

SFT Implementation We use the LLaMA-Factory (Zheng et al., 2024) implementation for our SFT experiments. By default, we adopt the SFT hyperparameters suggested by OpenThought3 (Guha et al., 2025) for medium dataset scales for the scenario that the base model evolves into LRMs, as shown below. To improve training efficiency, we employ FlashAttention-2 (Dao, 2023), DeepSpeed ZeRO-1 (Rasley et al., 2020), Liger kernels (Hsu et al., 2024), and asynchronous activation offloading (Daniel Han & team, 2023).

Training type	Batch Size	Context Length	LR	Epochs	LR Scheduler	Warmup Ratio	Weight Decay	Training Precision
Full	128	32,768	4e-5	5	cosine	0.1	0	bf16

For the extensive contamination to LRMs in the final stage, we use the hyperparameters as follows:

Training type	Batch Size	Context Length	LR	Epochs	LR Scheduler	Warmup Ratio	Weight Decay	Training Precision
Full	32	32,768	1e-5	7	cosine	0.1	0	bf16

RL Implementation We use Verl (Sheng et al., 2024) implementation for our RL experiments. For RAFT and RAFT++, we follow the implementation of (Xiong et al., 2025). For GRPO, we follow DAPO (Yu et al., 2025) and do not introduce the KL term in our training in all the experiments. The detailed hyperparameters are as follows:

Training type	Batch Size	Prompt Length	Response Length	ϵ	LR	Epochs	Rollout Num	Rollout Temp	Training Precision
Full	64	1,024	16,384	0.2	1e-6	1	4	0.6	bf16

Prompt template We use a prompt template to enable long CoT during train on both SFT and RL. We use math template to AIME2024 & 2025, AMC2023, OlympiadBench (He et al., 2024), and Minervamath (Lewkowycz et al., 2022). We adapt multiple-choice template to GPQA Diamond (Rein et al., 2024).

Evaluation and Metric We evaluate pass@1 and run 10 rollouts on AIME 2024 & 2025, AMC 2023, and 3 rollouts on OlympiadBench, GPQA Diamond, and Minerva Math to compute the pass@1. We use vLLM (Kwon et al., 2023) for the inference. All inference uses the same configurations: temperature=0.6, top_p=0.95, max_new_tokens=32,768.

Reasoning Template for Math

```
{question}\nPlease reason step by step, and put your final answer
within \boxed{}.
```

Example. Alice and Bob play the following game. A stack of n tokens lies before them. The players take turns with Alice going first. On each turn, the player removes either 1 token or 4 tokens from the stack. Whoever removes the last token wins. Find the number of positive integers n less than or equal to 2024 for which there exists a strategy for Bob that guarantees that Bob will win the game regardless of Alice's play.\nPlease reason step by step, and put your final answer within \boxed{}.

Deduplication We deduplicate our clean training datasets for both RL and SFT against the evaluation benchmarks using 13-gram overlap deduplication to ensure conclusive results.

Reasoning Template for Multiple Choice Question

```
Return your final response within \boxed{} and only include
the letter choice (A, B, C, or D) as your final response.
{question}{options}
```

Example.

```
Return your final response within \boxed{} and only
include the letter choice (A, B, C, or D) as your final response.
trans-cinnamaldehyde was treated with methylmagnesium bromide,
forming product 1.
1 was treated with pyridinium chlorochromate, forming product 2.
3 was treated with (dimethyl(oxo)-l6-sulfaneylidene)methane in DMSO
at elevated temperature, forming product 3.
how many carbon atoms are there in product 3?  A) 11, B) 10, C) 12,
D) 14
```

F More Experiment Results

F.1 More results of Llama-3.1-8B-Instruct (Stage I: pre-LRM)

Table 7: **AUROC (%)** of contamination detection approaches evaluated starting from an **SFT-contaminated model w/o RL to subsequently trained with GRPO**. Results demonstrate that after GRPO, AUROC decreases across all the benchmarks and detection approaches. Δ measures the difference with the SFT-contaminated model w/o RL. Higher AUROC, better detection performance. Each AUROC is averaged over detection scores from 8 rollouts. The base model is Llama3.1-8B-Instruct.

Contamination Detection Methods	Training Stages	Olympiad	GPQA	AIME25	AIME24	Minerva	AMC23	Avg.	Δ
Generation based									
Verbatim (Wu et al., 2025)	Before RL	48.67	65.36	51.78	60.00	56.84	52.62	55.88	+0.00
	RL w/ Clean	49.92	50.14	57.78	58.22	57.21	57.38	55.11	-0.77
	RL w/ Clean&Mem	48.42	48.21	54.89	56.22	57.83	58.00	53.93	-1.95
CDD (Dong et al., 2024)	Before RL	56.72	54.55	53.33	55.11	60.03	66.75	57.75	+0.00
	RL w/ Clean	53.14	55.69	60.00	46.22	56.31	64.00	55.89	-1.86
	RL w/ Clean&Mem	57.24	49.31	53.11	43.78	57.52	63.50	54.08	-3.67
Perturbation based									
Neighbor (Mattern et al., 2023)	Before RL	51.64	40.46	62.44	41.11	53.86	63.62	52.19	+0.00
	RL w/ Clean	52.48	37.07	55.78	39.33	50.32	65.00	50.00	-2.19
	RL w/ Clean&Mem	52.34	39.76	49.78	37.11	54.44	70.25	50.61	-1.58
Reference based									
LiRA (Mireshghallah et al., 2022)	Before RL	80.50	70.86	98.22	93.78	81.54	98.87	87.30	+0.00
	RL w/ Clean	68.95	65.57	51.33	41.11	73.99	80.75	63.62	-23.68
	RL w/ Clean&Mem	68.72	65.74	90.44	89.11	72.32	94.12	80.08	-7.22
Ref (Carlini et al., 2021)	Before RL	60.21	48.62	66.00	40.89	60.47	83.50	59.95	+0.00
	RL w/ Clean	55.27	47.41	40.67	32.44	52.31	53.25	46.89	-13.06
	RL w/ Clean&Mem	55.49	50.37	46.00	31.11	52.98	62.50	49.74	-10.21
Reference free									
Zlib (Carlini et al., 2021)	Before RL	49.46	56.21	88.44	72.00	47.04	60.25	62.23	+0.00
	RL w/ Clean	46.53	56.37	66.67	50.00	45.91	41.38	51.14	-11.09
	RL w/ Clean&Mem	47.29	52.29	66.22	60.89	45.63	46.00	53.05	-9.18
Min–K%++ (Zhang et al., 2024)	Before RL	48.88	49.33	41.43	39.11	51.67	30.63	43.51	+0.00
	RL w/ Clean	46.67	47.61	29.33	24.22	59.85	34.38	40.34	-3.17
	RL w/ Clean&Mem	48.08	50.65	36.22	28.44	59.27	46.63	44.88	+1.37
Min–K% (Shi et al., 2023)	Before RL	68.90	72.17	98.22	99.56	76.16	94.50	84.92	+0.00
	RL w/ Clean	59.11	69.85	60.44	67.56	73.89	75.87	67.79	-17.13
	RL w/ Clean&Mem	60.41	63.87	87.33	89.56	73.57	84.50	76.54	-8.38
Max–K% (Maini et al., 2024)	Before RL	63.60	61.58	92.44	89.33	69.12	91.50	77.93	+0.00
	RL w/ Clean	50.59	52.50	50.00	50.00	50.37	52.50	50.99	-26.94
	RL w/ Clean&Mem	50.91	52.24	49.11	49.11	54.86	61.75	53.00	-24.93
Loss (Carlini et al., 2021)	Before RL	69.44	72.88	98.67	99.56	76.91	94.50	85.33	+0.00
	RL w/ Clean	59.18	69.84	60.00	68.00	74.02	76.75	67.97	-17.36
	RL w/ Clean&Mem	60.37	63.92	89.33	90.44	74.18	84.62	77.14	-8.19

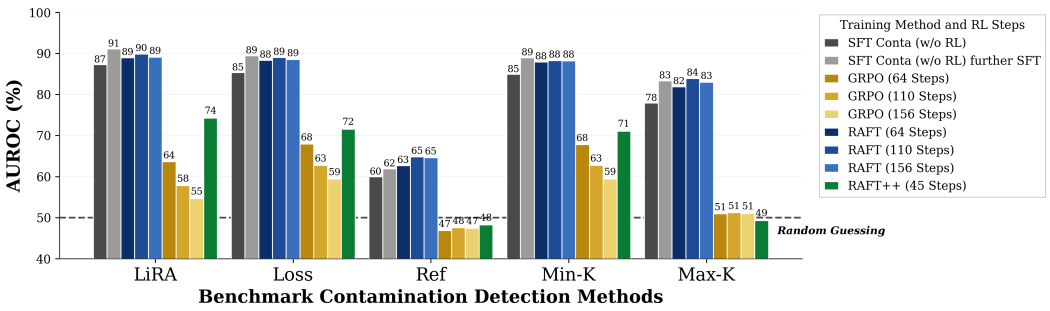

Figure 5: **AUROC (%) trends on SFT contaminated model further trained with different objectives.** While contamination introduced through SFT is initially detectable by existing methods, subsequent RL training with clean samples (e.g., GRPO or RAFT++) consistently degrades detection performance. Moreover, we observe a monotonic decline in detection performance as the number of RL steps increases, and reference-free methods (e.g., Loss, Min-K, and Max-K) already fall into near random guesses (i.e., AUROC≈50%) simply after 156 steps. The base model is Llama3.1-8B-Instruct.

F.2 AUROC ON QUESTION, QUESTION+RESPONSE, THINKING PROCESS, AND NON-THINKING PROCESS (STAGE I: PRE-LRM)

We compare the AUROC computed on response tokens with computed on the question tokens, whole tokens, thinking tokens, and non-thinking tokens in the response. As shown in Tab. 8 and 11, none of the approach outperform the AUROC computed on the response tokens. Thus, we choose to compute all the detection scores on the response if applicable. The base model here is Qwen2.5-7B-Instruct.

Table 8: AUROC (%) of contamination detection approaches using **question tokens** to compute the detection score, evaluated on the SFT-contaminated model w/o RL. Δ measures the difference with the **reponse tokens** as signal (Tab. 2). Results demonstrate that question tokens are not suitable for detection in the LRM contamination setting, compared with using response tokens.

Contamination Detection Methods	Olympiad	GPQA	AIME25	AIME24	Minerva	AMC23	Avg.	Δ
Generation base								
Verbatim (Wu et al., 2025)	47.58	49.86	47.56	53.56	52.52	65.50	52.76	+0.00
Perturbation base								
Neighbor (Mattern et al., 2023)	47.04	56.10	44.22	32.44	49.99	54.62	47.40	-3.31
Reference base								
LiRA (Mireshghallah et al., 2022)	49.78	43.12	42.22	46.00	48.77	55.00	47.48	-41.65
Ref (Carlini et al., 2021)	49.80	48.47	40.22	47.56	49.38	53.88	48.22	-17.28
Reference free								
Zlib (Carlini et al., 2021)	48.15	50.78	60.00	40.89	54.23	52.75	51.13	-2.25
Min–K%++ (Zhang et al., 2024)	44.33	50.53	32.00	36.89	49.67	34.25	41.28	-8.33
Min–K% (Shi et al., 2023)	46.68	51.91	53.33	43.56	54.13	44.38	49.00	-15.96
Max–K% (Maini et al., 2024)	49.39	54.58	71.56	55.33	54.98	66.25	58.68	-11.15
Loss (Carlini et al., 2021)	47.38	54.03	58.44	46.00	55.61	52.00	52.24	-23.24

F.3 RESPONSE LENGTH ANALYSIS (STAGE I: PRE-LRM)

We visualize the average response length per question across different benchmarks in Fig. 6. Here, the base model is Qwen2.5-7B-Instruct. Although the average response length does not change too much after GRPO training, several detection approaches already exhibit a substantial performance drop, as shown in Tab. 2. In contrast, for RAFT, even though the response lengths remain similar to those after GRPO, no concealment effect is observed. These results suggest that response length is not the key factor; instead, the entropy of the model's output appears to drive the concealment phenomenon.

Table 9: AUROC (%) of contamination detection approaches using **question + response tokens** to compute the detection score, evaluated on the SFT-contaminated model w/o RL. Δ measures the difference with **response tokens** as signal (Tab. 2). Results demonstrate that considering both question and response tokens when computing detection scores actually harms the AUROC.

Contamination Detection Methods	Olympiad	GPQA	AIME25	AIME24	Minerva	AMC23	Avg.	Δ
Perturbation base								
Neighbor (Mattern et al., 2023)	54.56	43.42	48.89	38.44	56.09	61.50	50.48	-0.23
Reference base								
LiRA (Mireshghallah et al., 2022)	79.31	72.49	89.56	71.11	66.07	89.00	77.92	-11.21
Ref (Carlini et al., 2021)	72.95	64.91	60.89	40.00	72.36	82.25	65.56	+0.06
Reference free								
Zlib (Carlini et al., 2021)	46.96	54.24	69.33	41.11	43.31	42.00	49.49	-3.89
Min–K%++ (Zhang et al., 2024)	40.49	51.08	36.19	48.67	39.61	30.50	41.09	-8.52
Min–K% (Shi et al., 2023)	56.46	56.73	85.78	73.78	48.48	58.13	63.23	-1.73
Max–K% (Maini et al., 2024)	64.43	63.78	64.22	81.78	66.09	76.50	69.47	-0.36
Loss (Carlini et al., 2021)	59.18	58.44	87.11	76.44	49.75	63.12	65.67	-9.81

Table 10: AUROC (%) of contamination-detection methods using **reasoning tokens only** (tokens inside `<think></think>`) to compute the detection score, evaluated on the SFT-contaminated model w/o RL. The last column, Δ, reports the difference relative to using **the entire response** as the signal (Tab. 2). Results show only minor differences between reasoning token only and whole-response signals, so we use the entire response in the main analysis.

Contamination Detection Methods	Olympiad	GPQA	AIME25	AIME24	Minerva	AMC23	Avg.	Δ
Reference free								
Zlib (Carlini et al., 2021)	49.67	59.60	70.89	35.24	48.60	46.00	51.67	-0.93
Min–K% (Shi et al., 2023)	70.76	66.46	82.89	74.52	70.34	82.25	74.54	+0.69
Max–K% (Maini et al., 2024)	67.40	62.00	66.67	82.38	65.87	79.00	70.55	+0.82
Loss (Carlini et al., 2021)	70.81	66.75	84.89	74.52	70.06	82.75	74.96	+1.21

Table 11: AUROC (%) of contamination-detection methods using **non-reasoning tokens only** (tokens after `</think>`) to compute the detection score, evaluated on the SFT-contaminated model w/o RL. The last column, Δ, reports the difference relative to using **the entire response** as the signal (Tab. 2). Results show that using non-reasoning tokens degrades performance compared with whole-response signals, so we use the entire response in the main analysis.

Contamination Detection Methods	Olympiad	GPQA	AIME25	AIME24	Minerva	AMC23	Avg.	Δ
Reference free								
Zlib (Carlini et al., 2021)	59.73	51.49	49.11	61.67	63.37	74.25	59.94	+7.34
Min–K% (Shi et al., 2023)	59.26	54.82	48.22	80.00	64.8	76.5	63.93	-9.92
Max–K% (Maini et al., 2024)	60.86	54.93	55.33	69.52	59.76	77.5	62.98	-6.75
Loss (Carlini et al., 2021)	59.28	54.78	48.44	80.00	64.74	76.5	63.96	-9.79

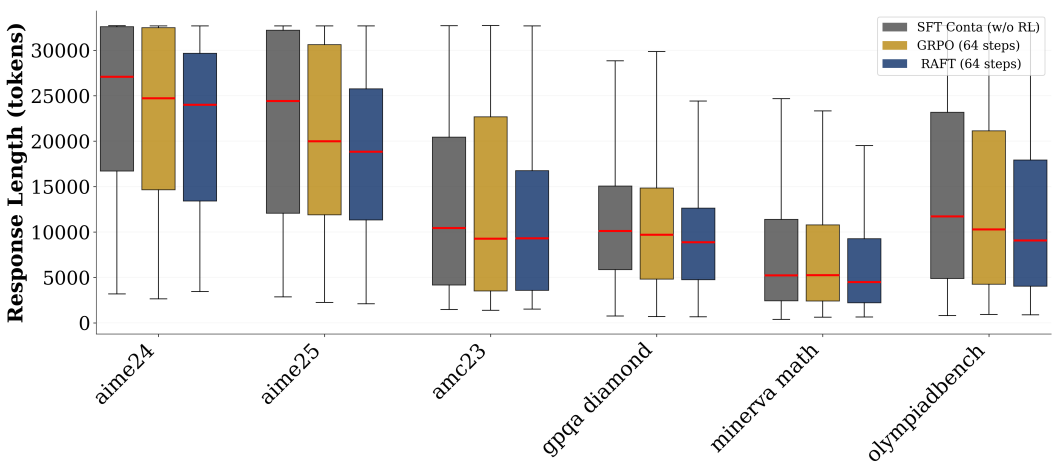

Figure 6: Average response length for each question across different benchmarks.

F.4 Log-probability distribution before and after RL (Stage I: pre-LRM)

We provide the log probability distribution for members vs. non-members in diverse scenarios. Fig. 7, 8, and 9 demonstrate that further SFT and RAFT are unable to contract the distribution for members and non-members, while GRPO and RAFT++ could conceal the contamination evidence due to the PPO-style importance sampling/clipping term in the training objective. The base model here is Qwen2.5-7B-Instruct.

F.5 AUROC for different training steps (Stage I: pre-LRM)

We provide complete results of AUROC in different RL training steps. As shown in Tab. 12 and 13, we observe a monotonic decline in detection performance as the number of RL steps increases when using GRPO. While even with 156 steps in RAFT, there is no sign of AUROC decline. These results perfectly validate our theoretical analysis that RAFT is unable to conceal contamination, while GRPO could.

F.6 Contamination Inflation Comparison (Stage I: pre-LRM)

To demonstrate performance inflation from SFT contamination, we choose Qwen2.5-7B-Instruct as the base model and compare pass@1 across three training settings: (i) 15K clean samples from Openthought3 (Guha et al., 2025), (ii) 10K clean samples plus three full repetitions of six entire benchmark data (13,735 samples in total), and (iii) 1.2M clean samples (i.e., open-thoughts/OpenThoughts3-1.2M). As shown in Tab. 16, the contaminated model outperforms the 15K clean baseline by an average of 10.80% across six benchmarks and even surpasses OpenThoughts3-1.2M on GPQA-Diamond and Minerva Math datasets. These results demonstrate that benchmark contamination can easily yield substantial performance inflation.

F.7 Log-prob distribution after extensive SFT contamination on LRMs (Stage II: post-LRM)

We provide the log prob distributions for members and non-members of deepseek distill models before and after contamination on Minvera Math and GPQA-Diamond in Fig. 10 and 11. Even though non-members have not been exposed to LRMs during the contamination, the log-prob would also increase, demonstrating that LRMs start to generalize after contamination.

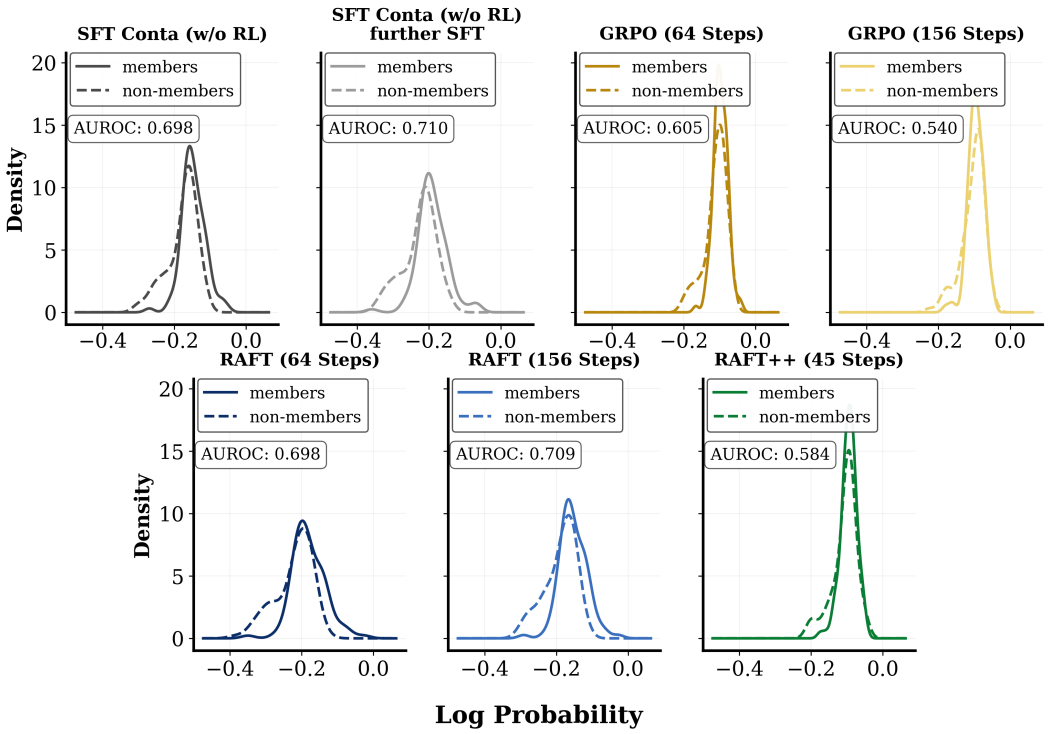

Figure 7: Log-prob distributions for members vs. non-members of **SFT contaminated model before and after RL training** on GPQA-Diamond. With additional GRPO or RAFT++ training on clean samples, the member and non-member log-probability distributions become increasingly similar. Since many contamination detection methods rely on separability in this space, the shrinking gap explains their degraded effectiveness. In contrast, further RAFT training does not induce the earlier distribution collapse; as we explain in Sec. 3.2, the absence of a clipping term prevents it. Likewise, additional SFT does not collapse the membership distributions.

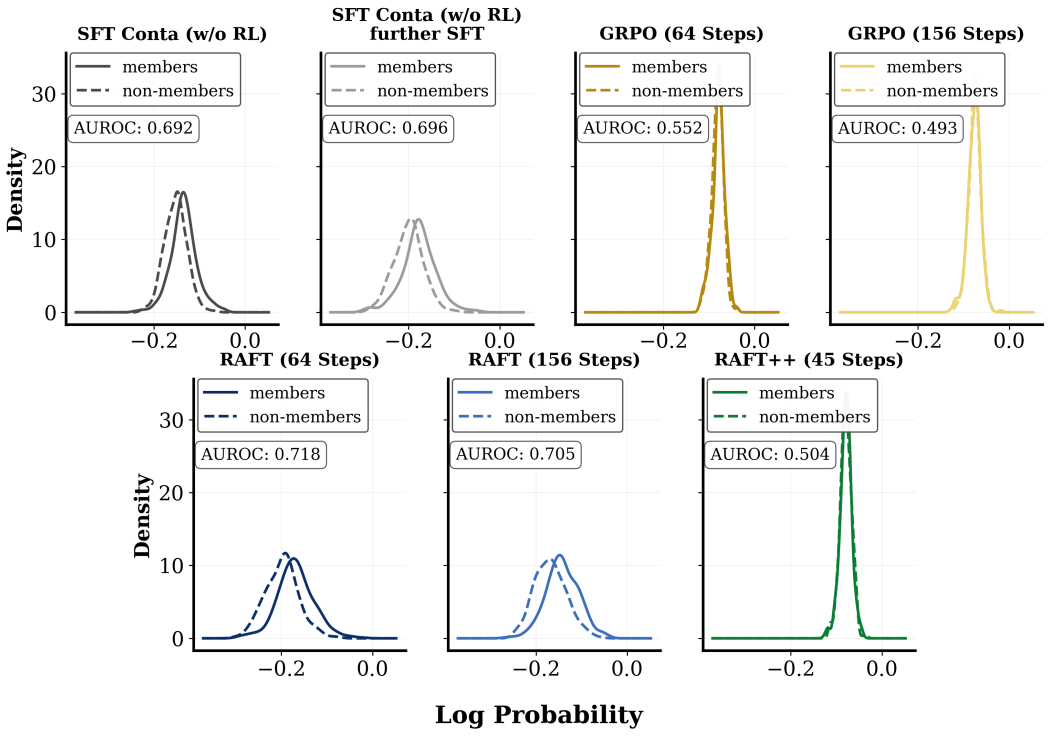

Figure 8: Log-prob distributions for members vs. non-members of **SFT contaminated model before and after RL training** on OlympiadBench. With additional GRPO or RAFT++ training on clean samples, the member and non-member log-probability distributions become increasingly similar. Since many contamination detection methods rely on separability in this space, the shrinking gap explains their degraded effectiveness. In contrast, further RAFT training does not induce the earlier distribution collapse; as we explain in Sec. 3.2, the absence of a clipping term prevents it. Likewise, additional SFT does not collapse the membership distributions.

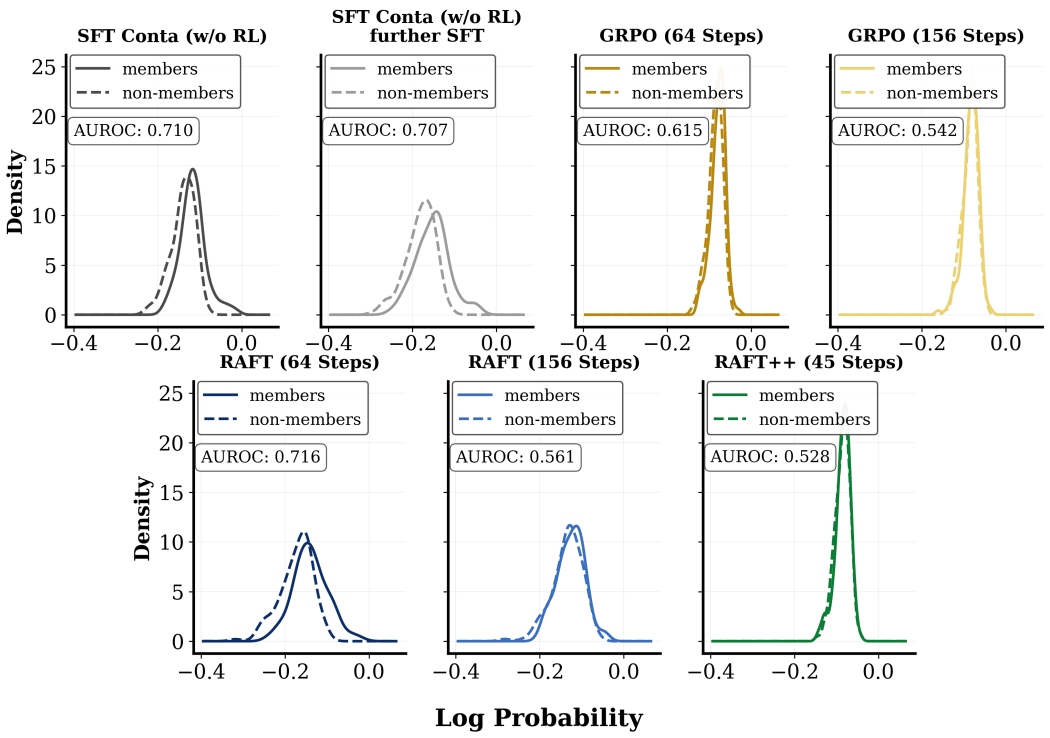

Figure 9: Log-prob distributions for members vs. non-members of **SFT contaminated model before and after RL training** on Minerva Math. With additional GRPO or RAFT++ training on clean samples, the member and non-member log-probability distributions become increasingly similar. Since many contamination detection methods rely on separability in this space, the shrinking gap explains their degraded effectiveness. In contrast, further RAFT training does not induce the earlier distribution collapse; as we explain in Sec. 3.2, the absence of a clipping term prevents it. Likewise, additional SFT does not collapse the membership distributions.

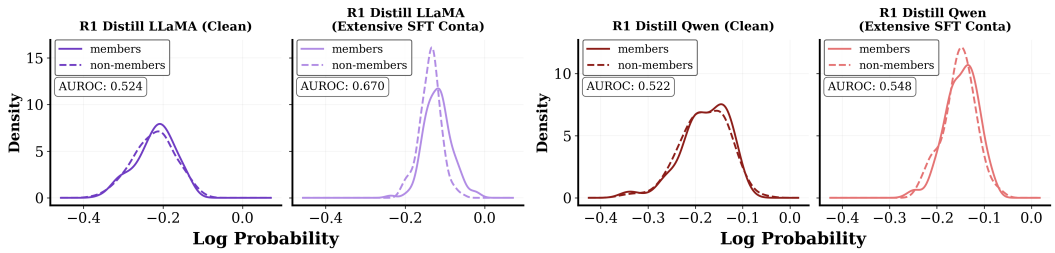

(a) R1 Distill LLaMA results on Minerva Math

(b) R1 Distill Qwen results on Minerva Math

Figure 10: Log-prob distributions for members vs. non-members of **advanced LRMs before and after contamination.** After extensive SFT contamination on members, the log prob of both members and non-members increases at a similar margin, due to the generalization.

Table 12: AUROC (%) of contamination detection approaches evaluated starting from an SFT-contaminated model w/o RL to subsequently trained with **GRPO in different steps**. Δ measures the difference with the SFT contaminated model w/o RL (Tab. 2). The results demonstrate that additional GRPO steps better conceal the contamination evidence. The base model here is Qwen2.5-7B-Instruct.

Contamination Detection Methods	Steps	Olympiad	GPQA	AIME25	AIME24	Minerva	AMC23	Avg.	Δ
Generation base									
Verbatim (Wu et al., 2025)	64	45.46	50.49	48.89	57.56	52.74	59.63	52.46	-0.30
	110	45.27	52.32	52.44	50.22	50.86	60.88	52.00	-0.76
	156	46.51	51.09	53.33	53.56	52.84	58.50	52.64	-0.12
CDD (Dong et al., 2024)	64	55.47	51.08	43.33	60.00	60.18	62.00	55.34	-0.45
	110	54.90	54.20	49.33	59.11	53.48	58.88	54.98	-0.81
	156	53.99	43.42	34.22	70.89	56.32	62.38	53.54	-2.25
Perturbation base									
Neighbor (Mattern et al., 2023)	64	54.10	39.68	50.67	44.22	53.42	60.5	50.43	-0.28
	110	53.93	40.93	43.11	46.22	54.27	59.62	49.68	-1.03
	156	53.32	41.07	47.11	38.67	54.49	60.75	49.24	-1.47
Reference base									
LiRA (Mireshghallah et al., 2022)	64	74.41	84.65	70.22	87.78	81.04	82.75	80.14	-8.99
	110	67.87	79.80	60.22	78.89	81.49	71.88	73.36	-15.77
	156	66.41	77.28	54.22	80.22	77.62	75.13	71.81	-17.32
Ref (Carlini et al., 2021)	64	66.77	58.41	45.33	51.11	65.54	73.62	60.13	-5.37
	110	64.92	54.70	44.44	52.22	66.47	72.37	59.19	-6.31
	156	62.20	57.30	50.89	55.78	64.62	75.25	61.01	-4.49
Reference free									
Zlib (Carlini et al., 2021)	64	45.94	54.99	66.22	35.56	46.65	39.38	48.12	-5.26
	110	44.98	56.54	64.22	39.11	44.93	38.38	48.03	-5.35
	156	44.82	53.21	63.11	41.33	46.43	39.12	48.00	-5.38
Min–K%++ (Zhang et al., 2024)	64	46.25	46.78	36.67	50.89	51.35	29.62	43.59	-6.02
	110	43.17	44.69	28.33	50.00	49.44	46.25	43.65	-5.96
	156	46.12	44.86	32.44	44.00	53.39	35.38	42.70	-6.91
Min–K% (Shi et al., 2023)	64	55.19	60.60	62.89	65.56	61.50	61.87	61.27	-13.69
	110	49.98	58.49	61.78	61.33	56.20	49.00	56.13	-18.83
	156	49.17	54.14	44.67	54.44	53.97	48.75	50.86	-24.10
Max–K% (Maini et al., 2024)	64	53.05	51.43	49.78	50.22	51.84	57.75	52.35	-17.48
	110	51.02	51.39	49.78	53.33	51.88	47.50	50.82	-19.01
	156	49.81	53.31	50.00	50.22	51.52	55.00	51.64	-18.19
Loss (Carlini et al., 2021)	64	55.22	60.50	62.44	65.78	61.50	62.12	61.26	-14.22
	110	50.17	58.25	60.67	62.89	56.47	49.12	56.26	-19.22
	156	49.32	54.04	44.22	54.22	54.20	48.50	50.75	-24.73

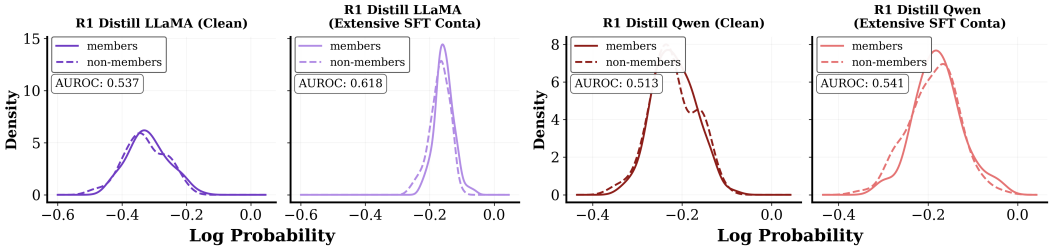

(a) R1 Distill LLaMA results on GPQA-Diamond (b) R1 Distill Qwen results on GPQA-Diamond

Figure 11: Log-prob distributions for members vs. non-members of **advanced LRMs before and after contamination.** After extensive SFT contamination on members, the log prob of both members and non-members increases at a similar margin, due to the generalization.

Table 13: AUROC (%) of contamination detection approaches evaluated starting from an SFT-contaminated model w/o RL to subsequently trained with **RAFT in different steps**. Δ measures the difference with the SFT contaminated model w/o RL (Tab. 2). Results demonstrate that even with more RL steps, RAFT is unable to conceal the contamination evidence. The base model here is Qwen2.5-7B-Instruct.

Contamination Detection Methods	Steps	Olympiad	GPQA	AIME25	AIME24	Minerva	AMC23	Avg.	Δ
Generation base									
Verbatim (Wu et al., 2025)	64	45.43	51.19	59.33	60.67	51.48	61.13	54.87	+2.11
	110	45.67	51.24	58.67	58.67	52.33	57.50	54.01	+1.25
	156	45.15	52.16	59.11	59.33	51.28	61.25	54.71	+1.95
CDD (Dong et al., 2024)	64	57.85	53.55	46.89	60.22	59.63	66.62	57.46	+1.67
	110	55.97	52.86	43.11	52.89	56.45	58.25	53.26	-2.53
	156	55.59	52.94	32.22	53.11	55.84	67.62	52.89	-2.90
Perturbation base									
Neighbor (Mattern et al., 2023)	64	55.44	39.63	50.22	43.11	53.15	58.88	50.07	-0.64
	110	55.06	38.47	46.89	40.67	54.20	63.38	49.78	-0.93
	156	55.06	39.19	40.89	41.78	49.66	57.12	47.28	-3.43
Reference base									
LiRA (Mireshghallah et al., 2022)	64	85.85	85.69	98.22	84.22	84.86	91.75	88.43	-0.70
	110	84.32	85.76	94.44	88.44	84.55	91.25	88.13	-1.00
	156	83.32	86.57	94.44	82.00	58.73	86.63	81.95	-7.18
Ref (Carlini et al., 2021)	64	76.02	65.94	74.67	46.00	73.99	75.62	68.71	+3.21
	110	76.41	63.76	71.11	50.22	74.50	81.75	69.63	+4.13
	156	75.92	64.23	67.33	54.67	56.73	81.38	66.71	+1.21
Reference free									
Zlib (Carlini et al., 2021)	64	51.88	59.73	76.00	52.22	52.40	47.75	56.66	+3.28
	110	52.39	62.20	76.22	49.78	74.51	45.88	56.29	+2.91
	156	53.04	62.35	79.78	47.78	52.58	50.37	57.65	+4.27
Min–K%++ (Zhang et al., 2024)	64	51.14	54.13	51.78	62.00	59.86	52.75	55.28	+5.67
	110	52.30	55.56	56.67	62.14	55.00	49.50	55.20	+5.59
	156	51.26	59.72	61.19	58.44	52.53	63.12	57.71	+8.10
Min–K% (Shi et al., 2023)	64	72.28	69.56	88.44	86.67	71.63	78.88	77.91	+2.95
	110	71.44	73.69	78.67	90.22	70.45	77.62	77.02	+2.06
	156	70.76	71.12	84.00	80.67	56.12	79.38	73.68	-1.28
Max–K% (Maini et al., 2024)	64	68.11	68.37	68.44	90.67	69.21	80.50	74.22	+4.39
	110	67.97	68.16	65.78	92.44	69.00	76.75	73.35	+3.52
	156	69.14	68.30	69.33	90.67	58.06	76.00	71.92	+2.09
Loss (Carlini et al., 2021)	64	71.78	69.78	86.00	86.67	71.58	79.25	77.51	+2.03
	110	71.09	73.54	78.44	91.11	70.13	77.12	76.90	+1.42
	156	70.49	70.95	83.11	80.44	56.07	79.12	73.36	-2.12

Table 14: AUROC (%) of contamination detection approaches evaluated starting from an SFT-contaminated model w/o RL to subsequently trained with **GRPO in different steps**. Δ measures the difference with the SFT contaminated model w/o RL (Tab. 7). The results demonstrate that additional GRPO steps better conceal the contamination evidence. The base model here is Llama-3.1-8B-Instruct.

Contamination Detection Methods	Steps	Olympiad	GPQA	AIME25	AIME24	Minerva	AMC23	Avg.	Δ
Generation base									
Verbatim (Wu et al., 2025)	64	49.92	50.14	57.78	58.22	57.21	57.38	55.11	-0.77
	110	49.53	51.25	54.22	60.67	54.73	53.12	53.92	-1.96
	156	49.45	52.11	51.11	60.44	57.02	47.12	52.88	-3.00
CDD (Dong et al., 2024)	64	53.14	55.69	60.00	46.22	56.31	64.00	55.89	-1.89
	110	53.48	48.40	46.67	49.11	57.34	56.00	51.83	-5.92
	156	53.99	52.18	45.56	52.89	60.62	57.25	53.75	-4.00
Perturbation base									
Neighbor (Mattern et al., 2023)	64	52.48	37.07	55.78	39.33	50.32	65.00	50.00	-2.19
	110	52.83	38.31	49.78	39.56	50.18	60.00	48.44	-3.75
	156	53.09	39.15	48.00	44.00	52.29	62.25	49.80	-2.39
Reference base									
LiRA (Mireshghallah et al., 2022)	64	68.95	65.57	51.33	41.11	73.99	80.75	63.62	-23.68
	110	66.57	65.72	44.22	27.56	72.02	71.00	57.85	-29.45
	156	60.93	64.21	40.22	23.11	69.25	70.12	54.64	-32.66
Ref (Carlini et al., 2021)	64	55.27	47.41	40.67	32.44	52.31	53.25	46.89	-13.06
	110	54.98	49.70	42.89	26.67	53.16	58.00	47.57	-12.38
	156	53.23	47.75	43.11	27.33	56.31	56.75	47.41	-12.54
Reference free									
Zlib (Carlini et al., 2021)	64	46.53	56.37	66.67	50.00	45.91	41.38	51.14	-11.09
	110	46.78	57.11	64.89	48.44	46.40	37.25	50.15	-12.08
	156	46.32	54.41	65.78	39.78	42.50	42.88	48.61	-13.62
Min–K%++ (Zhang et al., 2024)	64	46.67	47.61	29.33	24.22	59.85	34.38	40.34	-3.17
	110	49.92	50.25	42.89	27.78	57.32	42.75	45.15	+1.64
	156	49.42	48.28	41.33	38.67	53.09	48.25	46.51	+3.00
Min–K% (Shi et al., 2023)	64	59.11	69.85	60.44	67.56	73.89	75.87	67.79	-17.13
	110	56.75	66.89	54.89	64.22	71.61	62.25	62.77	-22.15
	156	55.83	65.12	50.44	59.78	62.76	62.50	59.41	-25.51
Max–K% (Maini et al., 2024)	64	50.59	52.50	50.00	50.00	50.37	52.50	50.99	-26.94
	110	50.29	54.44	50.00	50.00	50.00	52.50	51.21	-26.72
	156	50.30	51.41	53.33	50.00	51.09	50.00	51.02	-26.91
Loss (Carlini et al., 2021)	64	59.18	69.84	60.00	68.00	74.02	76.75	67.97	-17.36
	110	56.85	66.90	55.11	63.78	71.60	62.38	62.77	-22.56
	156	55.75	65.06	50.00	59.78	62.72	63.00	59.39	-25.94

Table 15: AUROC (%) of contamination detection approaches evaluated starting from an SFT-contaminated model w/o RL to subsequently trained with **RAFT in different steps**. Δ measures the difference with the SFT contaminated model w/o RL (Tab. 7). Results demonstrate that even with more RL steps, RAFT is unable to conceal the contamination evidence. The base model here is Llama-3.1-8B-Instruct.

Contamination Detection Methods	Steps	Olympiad	GPQA	AIME25	AIME24	Minerva	AMC23	Avg.	Δ
Generation base									
Verbatim (Wu et al., 2025)	64	46.75	49.07	56.44	58.89	55.77	57.00	53.99	-1.89
	110	46.89	50.85	52.00	53.33	58.78	55.12	52.83	-3.05
	156	47.06	49.70	54.22	60.44	55.63	61.75	54.80	-1.08
CDD (Dong et al., 2024)	64	57.35	54.44	52.22	46.44	53.57	62.62	54.44	-3.31
	110	56.97	54.92	60.00	50.00	55.76	65.38	57.17	-0.58
	156	55.78	57.84	53.11	50.89	60.63	70.88	58.19	+0.44
Perturbation base									
Neighbor (Mattern et al., 2023)	64	51.81	40.93	64.00	48.44	55.28	66.50	54.49	+2.30
	110	52.08	39.36	64.22	54.00	54.84	68.88	55.56	+3.37
	156	51.99	40.25	66.22	49.56	51.68	72.75	55.41	+3.22
Reference base									
LiRA (Mireshghallah et al., 2022)	64	81.82	77.88	96.89	96.67	82.92	97.50	88.95	+1.75
	110	81.54	77.08	99.56	95.78	86.03	99.00	89.83	+2.63
	156	80.52	77.21	99.11	96.00	84.04	97.75	89.11	+1.91
Ref (Carlini et al., 2021)	64	60.81	51.55	65.33	49.11	61.41	88.00	62.70	+2.75
	110	62.25	49.94	76.89	52.67	61.33	86.00	64.85	+4.93
	156	61.14	48.53	77.78	49.78	63.06	87.50	64.63	+4.68
Reference free									
Zlib (Carlini et al., 2021)	64	53.02	58.98	80.67	68.44	51.21	60.75	62.18	-0.05
	110	53.40	64.35	89.33	66.22	53.83	67.88	65.84	+3.61
	156	54.13	62.78	85.33	64.89	54.81	68.62	65.09	+2.86
Min–K%++ (Zhang et al., 2024)	64	48.97	48.15	36.00	36.89	55.41	37.25	43.78	+0.27
	110	51.00	56.82	44.44	38.89	58.25	39.47	48.15	+4.64
	156	50.43	58.89	34.44	29.11	58.98	45.50	46.23	+2.72
Min–K% (Shi et al., 2023)	64	73.95	76.84	98.00	98.89	82.44	97.25	87.90	+2.98
	110	71.87	80.78	98.89	98.22	83.92	95.88	88.26	+3.34
	156	71.30	81.59	98.22	100.00	82.54	95.50	88.19	+3.27
Max–K% (Maini et al., 2024)	64	66.57	70.43	92.44	89.11	77.31	95.25	81.85	+3.92
	110	67.37	75.39	92.89	92.00	78.65	96.88	83.86	+5.93
	156	67.61	73.85	90.67	94.22	76.10	95.50	82.99	+5.06
Loss (Carlini et al., 2021)	64	73.77	78.18	98.00	99.56	83.14	97.38	88.34	+3.01
	110	72.40	81.76	99.11	98.67	84.18	97.75	88.98	+3.65
	156	71.57	82.91	98.67	100.00	82.34	95.75	88.54	+3.21

Table 16: Pass@1 (%) of comparison between clean and contaminated SFT models. **Bold**=Best.

Training Data	Olypaid	GPQA	AIME25	AIME24	Minerva	AMC23	Avg.
15K clean	50.81	41.67	21.67	29.17	34.01	77.50	42.47
13.7K (clean + benchmarks)	58.52	**59.09**	40.00	40.00	**44.49**	77.50	53.27
1.2M clean	**63.70**	50.88	**60.00**	**62.50**	37.50	**92.50**	**61.18**

F.8 Token Embedding Visualization of member/non-member of benchmarks (Stage I: pre-LRM)

We provide UMAP visualization of token embeddings of member and non member of benchmarks. Specifically, we input the entire question and response to the model, and extract the last token from the last layer of the hidden space. The base model is selected as Qwen2.5-7B-Instruct. We choose n_neighbors as 15, min_dist as 0.1, n_components as 2, and metric as cosine. As shown in Fig. 12, 13, and 14, the visualization indicates that member/non-member embeddings are highly overlapped and are hard to distinguish. We also provide quantitative evaluations of embedding based detection following (Liu et al., 2024b) in Table 17. In particular, we randomly split all member and non-member examples into training and test sets, maintaining a consistent 0.8/0.2 ratio across datasets, and train an MLP classifier to predict the member/non-member labels. The input to the MLP is the hidden state feature of the last token in the question and response pair. Following (Liu et al., 2024b), we evaluated several hidden layers and selected the best performing one. We report results only on the medium-scale benchmarks (Olympiad, GPQA, Minerva), since the small-scale datasets have very few test examples, resulting in too much variance. The results show that contamination is initially detectable, but becomes undetectable after RL.

Table 17: AUROC (%) of the embedding-based detection (Liu et al., 2024b) evaluated starting from an SFT-contaminated model w/o RL to subsequently trained with GRPO. Results demonstrate that after GRPO, AUROC decreases. Δ measures the difference with the SFT-contaminated model w/o RL. Here, the base model is Qwen2.5-7B-Instruct.

Training Stage	Olympiad	GPQA	Minerva	Avg.	Δ
Before RL	58.89	80.00	60.05	66.31	+0.00
RL w/ Clean	56.63	45.75	49.60	50.66	-15.65
RL w/ Clean&Mem	57.43	45.00	48.94	50.46	-15.85

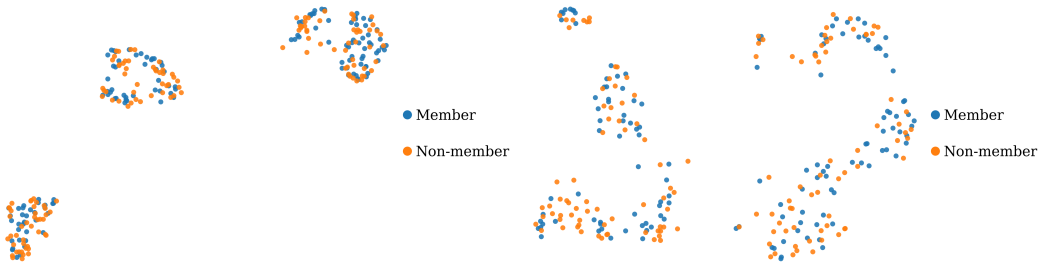

(a) Base model (b) SFT contaminated model

Figure 12: Last token embedding visualization on the Minerva Math dataset.

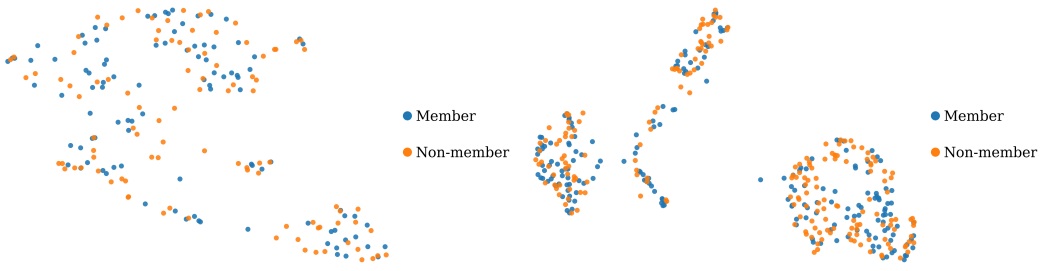

(a) Base model (b) SFT contaminated model

Figure 13: Last token embedding visualization on the GPQA-Diamond dataset.

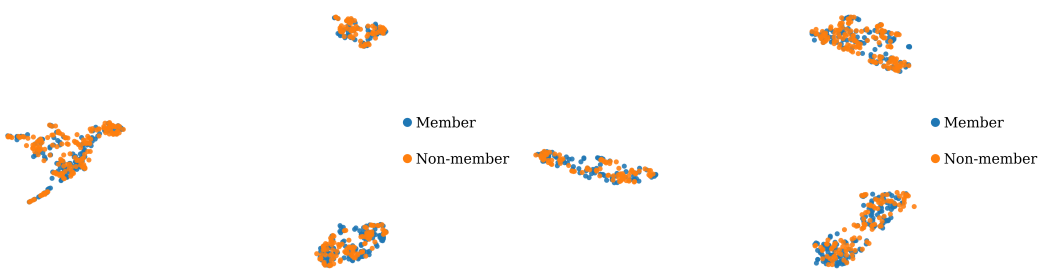

(a) Base model (b) SFT contaminated model

Figure 14: Last token embedding visualization on the OlympiadBench dataset

F.9 Applicability in non-math domains (Stage I and II)

We further evaluate our claims on datasets beyond math and science domains for both the pre-LRM and the post-LRM stage. We choose LiveCodeBench v2 (Coding) and MMLU-Pro (General QA). For MMLU-Pro, we only select the 'health', 'history', 'law', 'other', 'philosophy', and 'psychology' domains that are not related to math and science.

We first provide results for the pre-LRM stage (i.e., contamination happens when the base model evolves into LRMs) with Qwen2.5-7B-Instruct as the base model in Table 18. Despite differences in AUROC degradation speed across domains, the trend remains consistent: RL conceals the SFT contamination. Overall, these results indicate that the effect of RL concealments is not limited to the reasoning domains but extends to more general domains as well.

We also provide the AUROC of contamination detection approaches evaluated on advanced LRM that is contaminated in the post-LRM stage (i.e., contamination with CoT on advanced LRMs) in Table 19. The results show that contaminated LRMs leave minimal contamination evidence in coding as well, indicating that the detection performance is near random guess for those reasoning-related domains (e.g., coding, math, science, etc). For domains that require less CoT (e.g., general QA), despite that the AUROC could reach 75% when using the Loss as the detection for the contaminated Deepseek distilled Qwen-14B, the detection performance is much worse compared to results in the pre-LRM stage. Specifically, the AUROC for the Loss detector on MMLU-Pro can reach 93.72%, and LiRA could achieve 79.85% on LiveCodeBench when SFT contamination is applied to the base model, shown in Table 18 in the paper.

Table 18: **AUROC (%)** of contamination detection approaches evaluated starting from an SFT-contaminated model w/o RL to subsequently trained with GRPO **in pre-LRM stage**. Results demonstrate that after GRPO, AUROC decreases across **both general QA and coding domains** and different detection approaches. Δ measures the difference with the SFT-contaminated model w/o RL. Higher AUROC, better detection performance. The base model here is Qwen2.5-7B-Instruct.

Contamination Detection Methods	Training Stages	MMLU-Pro (Non-STEM domains)	LiveCodeBench	Avg.	Δ
Reference based					
LiRA (Mireshghallah et al., 2022)	Before RL	96.68	79.85	88.26	+0.00
	RL w/ clean	93.85	71.12	82.48	-5.78
Ref (Carlini et al., 2021)	Before RL	86.25	69.51	77.88	+0.00
	RL w/ clean	81.67	66.68	74.17	-3.71
Reference free					
Loss (Carlini et al., 2021)	Before RL	93.72	64.87	79.29	+0.00
	RL w/ clean	88.69	54.26	71.47	-7.82
Min–K (Shi et al., 2023)	Before RL	93.43	64.12	78.77	+0.00
	RL w/ clean	88.54	54.29	71.41	-7.36
Max–K (Maini et al., 2024)	Before RL	82.27	63.75	73.01	+0.00
	RL w/ clean	59.48	49.80	54.64	-18.37

Table 19: AUROC (%) of contamination detection approaches evaluated on advanced LRMs contaminated with CoT in both **general QA and coding domain** benchmarks **in post-LRM stage**.

Contamination Detection Methods	Init Models	MMLU-Pro (Non-STEM domains)	LiveCodeBench	Avg.
Reference based				
LiRA (Mireshghallah et al., 2022)	DS Llama-8B	72.85	61.37	67.11
	DS Qwen-14B	74.75	58.78	66.77
Ref (Carlini et al., 2021)	DS Llama-8B	60.77	58.75	59.76
	DS Qwen-14B	63.43	58.17	60.80
Reference free				
Loss (Carlini et al., 2021)	DS Llama-8B	69.56	57.42	63.49
	DS Qwen-14B	75.83	56.52	66.18
Min–K (Shi et al., 2023)	DS Llama-8B	68.12	56.59	62.36
	DS Qwen-14B	76.09	56.08	66.09
Max–K (Maini et al., 2024)	DS Llama-8B	61.07	56.33	58.70
	DS Qwen-14B	66.88	54.80	60.84

F.10 Contraction effect on small and large models (Stage I: pre-LRM)

We conduct experiments on smaller and larger models to see whether the concealment of RL has correlations with the model size. In particular, we provide additional results with a small model (i.e., Qwen2.5-3B-Instruct) in Table 20, and a large model (i.e., Qwen2.5-14B-Instruct) in Table 21. We compare them with the contraction of the medium-sized model (i.e., Qwen2.5-7B-Instruct). Here, RL steps are 64 by default. The empirical results further validate that the contraction extends to a large range of model sizes. Regardless of different model sizes, the RL training could still conceal the contamination introduced in the SFT stage.

Table 20: **AUROC (%)** of contamination detection approaches evaluated starting from an SFT-contaminated model w/o RL to subsequently trained with GRPO. Results demonstrate that after GRPO, AUROC decreases across all the benchmarks and detection approaches. Δ measures the difference with the SFT-contaminated model w/o RL. **The base model here is Qwen2.5-3B-Instruct.**

Contamination Detection Methods	Training Stages	Olympiad	GPQA	AIME25	AIME24	Minerva	AMC23	Avg.	Δ
Reference based									
LiRA (Mireshghallah et al., 2022)	Before RL	54.89	48.60	88.67	95.56	61.74	90.25	73.29	+0.00
	RL w/ Clean	53.93	51.17	62.89	81.56	60.10	81.50	65.19	-8.09
Ref (Carlini et al., 2021)	Before RL	52.66	43.09	84.00	73.33	51.75	75.75	63.43	+0.00
	RL w/ Clean	53.65	44.54	66.44	63.33	52.24	73.25	58.91	-4.52
Reference free									
Loss (Carlini et al., 2021)	Before RL	51.75	57.64	58.00	76.00	56.84	64.75	60.83	+0.00
	RL w/ Clean	49.20	57.54	42.22	55.11	54.83	54.75	52.28	-8.56
Min–K (Shi et al., 2023)	Before RL	50.86	57.24	51.11	73.33	56.47	59.13	58.02	+0.00
	RL w/ Clean	48.71	56.93	39.56	49.78	54.90	51.37	50.21	-7.82
Max–K (Maini et al., 2024)	Before RL	52.86	54.58	88.44	88.44	51.35	79.12	69.13	+0.00
	RL w/ Clean	52.07	54.54	56.67	57.78	52.57	74.00	57.94	-11.19

F.11 More RL training brings performance gain (Stage I: pre-LRM)

In Table 1, we note that sometimes RL does not bring any performance gain, even in the clean setting. To clarify that our RL setting and recipe are correct, we would like to point out that the insignificant RL improvement was due to our relatively short RL training run to save experiment cost, which already effectively demonstrated the contamination concealment effect, whereas RL fine-tuning on reasoning models typically requires many more training steps to boost performance significantly (i.e, thousands of RL steps, more than 16k GPU hours, etc).

However, we further verified our RL pipeline by continuing RL training on the SFT-contaminated Qwen-3B model for up to 280 steps. The RL concealment still exists: the average AUROC of LiRA on the AIME24, AIME25, and AMC23 datasets drops from 91.49% before RL to approaching random guessing after 280 steps. At the same time, RL continues to improve task performance,

Table 21: **AUROC (%)** of contamination detection approaches evaluated starting from an SFT-contaminated model w/o RL to subsequently trained with GRPO. Results demonstrate that after GRPO, AUROC decreases across all the benchmarks and detection approaches. Δ measures the difference with the SFT-contaminated model w/o RL. **The base model here is Qwen2.5-14B-Instruct.**

Contamination Detection Methods	Training Stages	Olympiad	GPQA	AIME25	AIME24	Minerva	AMC23	Avg.	Δ
Reference based									
LiRA (Mireshghallah et al., 2022)	Before RL	87.35	86.54	91.56	85.33	88.12	91.25	88.36	+0.00
	RL w/ Clean	83.46	82.38	90.56	84.00	82.23	84.88	84.59	-3.77
Ref (Carlini et al., 2021)	Before RL	62.33	54.69	60.44	37.78	59.26	65.25	56.63	+0.00
	RL w/ Clean	56.28	58.85	50.67	36.00	53.32	63.88	53.17	-3.46
Reference free									
Loss (Carlini et al., 2021)	Before RL	73.59	76.98	79.11	88.00	77.45	84.88	80.00	+0.00
	RL w/ Clean	63.50	61.21	67.33	89.11	71.73	68.75	70.27	-9.73
Min–K (Shi et al., 2023)	Before RL	73.04	76.16	77.11	86.22	77.61	83.75	78.98	+0.00
	RL w/ Clean	63.15	60.09	66.67	87.78	71.69	67.12	69.42	-9.57
Max–K (Maini et al., 2024)	Before RL	63.75	71.46	64.00	84.89	57.99	78.00	70.02	+0.00
	RL w/ Clean	52.94	59.10	46.67	53.33	48.89	55.00	52.66	-17.36

as reported in Table 22. Overall, these results demonstrate that additional RL training on an SFT-contaminated model can both inflate performance and further conceal contamination signals.

Table 22: **Pass@1 (%)** across six reasoning benchmarks. Results show that additional RL training on an SFT-contaminated model can bring performance gain.

Model	Olympiad	GPQA	AIME25	AIME24	Minerva	AMC23	Avg.
Qwen2.5-3B-Instruct	26.98	31.06	0.83	6.67	21.69	36.07	20.54
↪ SFT contamination	35.07	37.11	13.23	14.32	29.13	44.06	28.82
↪ Further RL	**40.74**	**38.38**	**15.12**	**15.83**	**31.25**	**49.06**	**31.73**

Table 23: Pass@1 (%) of the SFT-contaminated model after four additional epochs of SFT on clean data. The results show that further SFT does not make the model forget contamination; instead, pass@1 continues to increase by 0.25% across six benchmark on average compared to the SFT contaminated model, indicating persistent performance inflation.

Models	Olypaid	GPQA	AIME25	AIME24	Minerva	AMC23	Avg.
SFT Conta (w/o RL) + Further SFT	55.24	49.43	29.58	36.67	39.15	75.00	47.52

G Computation Resources

All experiments were run on a single node with 9× NVIDIA L40S GPUs (48 GiB each; ∼432 GiB total), NVIDIA driver 570.86.16, and CUDA 12.8. The node uses a 1-socket Intel Xeon Gold 6338 CPU (2.00 GHz base, up to 3.20 GHz), 128 hardware threads, 96 MiB L3 cache (two slices), and 1.0 TiB RAM, running Ubuntu 22.04 (Linux 6.8.0-79-generic).

Table 24: Pass@1 (%) of advanced LRMs before and after SFT contamination with CoT on both clean and member data. Some LRMs with strong reasoning ability may not have a huge performance inflation after SFT contamination with CoT on both clean and members. Thus, we choose the SFT contamination with CoT on members only as the default setup in our main analysis.

Models	Olypaid	GPQA	AIME25	AIME24	Minerva	AMC23	Avg.
DeepSeek-R1-Distill-Llama-8B	52.10	43.94	33.33	43.33	32.97	84.58	48.38
↪ SFT w/ Clean & Mem	56.70	45.83	48.33	56.67	35.94	88.12	55.27
DeepSeek-R1-Distill-Qwen-7B	55.70	48.65	39.26	53.70	37.25	91.94	54.42
↪ SFT w/ Clean & Mem	55.81	45.08	40.00	55.42	37.87	88.12	53.72